Analysis of an optimal control problem related to anaerobic digestion process

Térence Bayen, Olivier Cots, Pedro P. Gajardo

A geometric approach to a minimal time control problem related to anaerobic wastewater treatment process

Terence Bayen*†, Olivier Cots‡, Pedro Gajardo§

November 5, 2017

Abstract

Our aim in this work is to synthesize optimal feeding strategies maximizing over a time period the biogas production in a continuously filled bioreactor controlled by its dilution rate. Following [5], such an anaerobic process is described by the so-called *AM2 model* which is a four-dimensional dynamical system. Instead of modeling the optimization of the biogas production as an optimal control problem of Lagrange type, we propose in this paper a slightly different optimal control approach : we study the minimal time control problem to reach a target point which is chosen in such a way that it maximizes the biogas production in the AM2 model at steady state. Thanks to the Pontryagin Maximum Principle and to geometric control theory, we provide an optimal feedback control for the minimal time control problem when initial conditions are taken on the invariant and attractive manifold of the system. The optimal synthesis exhibits turnpike and anti-turnpike singular arcs and a cut-locus.

Keywords. Chemostat Model, Optimal Feedback, Geometric Control, Pontryagin Maximum Principle.

1 Introduction

Within the context of renewable energies, anaerobic digestion of waste and wasted water has become an attractive alternative to carbon fossil, being a well-known and established technology to treat waste in the methanization of sewage sludge from wastewater treatment plants [15]. Anaerobic digestion is a complex process that can take place in one bioreactor used for the production of biogas (methane, hydrogen). From a practical point of view, one main issue is to obtain an efficient management policy for anaerobic digestion processes in order to maximize the biogas outflow produced over a given period (see *e.g.* [12]).

A representation of this process is based on the coupling of two main reactions called acidogenesis and methanization. These two reactions can be described by the so-called *AM2 model* (see [5]) represented by the system:

$$\begin{cases} \dot{X}_1 &= \tilde{\mu}_1(S_1)X_1 - \alpha D X_1, \\ \dot{S}_1 &= -k_1\tilde{\mu}_1(S_1)X_1 + D(S_{in}^1 - S_1), \\ \dot{X}_2 &= \tilde{\mu}_2(S_2)X_2 - \alpha D X_2, \\ \dot{S}_2 &= k_2\mu_1(S_1)X_1 - k_3\tilde{\mu}_2(S_2)X_2 + D(S_{in}^2 - S_2), \end{cases} \tag{1.1}$$

that is based on the chemostat model (see [13, 16, 21]). Here, X_1, resp. X_2 stands for the concentration of acidogenic bacteria[1], resp. methanogenic bacteria, S_i, $i = 1, 2$ are the substrate concentrations, and D is the dilution rate of the continuously operated bioreactor (*i.e.*, $D = Q/V$ where Q is the input and output flow rate of water and V is the constant volume of water present in the bioreactor). The coefficient $\alpha \in (0, 1]$

*Institut Montpelliérain Alexander Grothendieck, CNRS, Université de Montpellier, France. terence.bayen@umontpellier.fr

†UMR INRA-SupAgro 729 'MISTEA' 2 place Viala 34060 Montpellier, France.

‡INP-ENSEEIHT, Université de Toulouse, IRIT & CNRS, 2 rue Camichel, F-31071 Toulouse, France olivier.cots@enseeiht

§Departamento de Matemática, Universidad Técnica Federico Santa María, Avenida España 1680, Valparaíso, Chile pedro.gajardo@usm.cl

[1]The signification of each variable is summarized in Table 1 in the Appendix (Section 7).

models the retention of biomass in the liquid phase, S_{in}^i, $i = 1, 2$ are the two input substrate concentrations, and $\tilde{\mu}_i(\cdot)$, $i = 1, 2$ are the two growth functions or kinetics for microorganisms X_1 and X_2.

In such process, the gas outflow produced in the fermentor is proportional to the production of methanogenesis species X_2. Over a time period $[0, T]$, the production of biogas in such process is then proportional to the quantity written in integral form :

$$\int_0^T \tilde{\mu}_2(S_2(t))X_2(t)\ \mathrm{d}t. \tag{1.2}$$

Finding an adequate functioning mode for which (1.2) is maximal then amounts to study an optimal control problem : one aims at finding an adequate feeding strategy maximizing (1.2) among solutions of (1.1) (here, the system (1.1) is controlled via the input flow rate $D(\cdot)$ that plays the role of the control function).

Optimal control theory is well suited to study such an optimization problem (via Pontryagin's Principle or Hamilton-Jacobi equation). However, in the present form, this optimal control problem presents several difficulties as for instance the curse of dimensionality when solving Hamilton-Jacobi equation associated to the optimal control problem, or the determination of a time dependent optimal feedback control for this problem. From a practical point of view, the knowledge of an autonomous feedback control would be more useful in order to pilot adequately a fermentor. In order to operate optimally such system, we propose an alternative way based on a two-step optimization procedure and that takes into account the previous remarks :

1. We first suppose the system at steady state, and we maximize the static production of biogas among equilibria of (1.1) *i.e.* the quantity $\tilde{\mu}_2(S_2)X_2$ among constant dilution rates. Following [1], this procedure allows us to obtain steady states of (1.1) maximizing the biogas production.

2. The second step consists in introducing a new optimal control problem governed by (1.1). We aim at finding an optimal feedback control driving (1.1) in minimal time to the target point defined as the optimal steady state in the previous problem.

Our aim in this work is to address essentially the second point using the theory of optimal control (the first point which consists in maximizing (1.2) among steady states of (1.1) was recently addressed in [1]). From a practical point of view, a reactor cannot be initiated at the optimal point due to uncertainties and to the initial conditions inside a fermentor. Thus, it is of particular interest to synthesize a feedback control strategy (in particular for robustness aspects) driving optimally the system to this operating point provided that this optimal point is known. When the desired target has been reached, the bioreactor can be then operated at the corresponding equilibrium which allows to have a guaranteed production of biogas over time.

The paper is organized as follows. In Section 2, we recall some properties of the AM2-model that are useful to transform (1.1) into a two-dimensional affine system with a drift and one input. We also recall a result of [1] (see Proposition 2.1) which shows that the target point maximizing the biogas production at steady state necessarily belongs to the collinearity curve of the system. This property appears to be an essential key point in this study. More precisely, considering a target point on the collinearity curve brings controllability issues and difficulties to exclude extremal trajectories that could cross this set several times. In Section 3, we apply the Pontryagin Maximum Principle, and we provide properties of the switching functions that will allow us to exclude extremal trajectories that are non optimal. We also give geometrical properties of the collinearity curve and of the singular locus. Finally, Section 4 provides optimality results and an optimal feedback control for the minimum time control problem to reach any target point chosen on the collinearity curve. The optimal synthesis is depicted in the context of the study of a fermentor described in [5] using the numerical values that were obtained experimentally from real measurements (see Appendix in Section 7). For each initial condition ξ_0 of the state space, we compute an optimal control $t \mapsto u(t, \xi_0)$ in open loop leading to the determination of an optimal feedback control $u[\xi_0] := u(0, \xi_0)$. The optimal synthesis exhibits a singular arc that has the property to be time-minimizing (*i.e.* a *turnpike*) in a subset of the state space whereas it is time-maximizing (*i.e.* an *anti-turnpike*) in its complementary. In the subset of the state space containing the anti-turnpike singular locus, optimal strategies can be non-unique, and we compute numerically a cut-locus using a homotopy method (see *e.g.* [10]).

2 Statement of the problem

2.1 Preliminaries on the modeling of a fermentor

In this section, we briefly recall the modeling of a two-step fermentor that will be useful to state the optimal control problem. Following [1], the model (1.1) proposed in [5], can be written as the following equivalent dynamical system

$$\begin{cases} \dot{x}_1 &= \mu_1(s_1)x_1 - ux_1, \\ \dot{s}_1 &= -\mu_1(s_1)x_1 + \frac{u}{\alpha}(s_{in}^1 - s_1), \\ \dot{x}_2 &= \mu_2(s_2)x_2 - ux_2, \\ \dot{s}_2 &= \mu_1(s_1)x_1 - \mu_2(s_2)x_2 + \frac{u}{\alpha}(s_{in}^2 - s_2), \end{cases} \tag{2.1}$$

after several change of variables indicated in Table 2 (see Appendix in Section 7).

This new model (with much less parameters) is still describing the two main coupled reactions (acidogenesis and methanization) of anaerobic digestion, inside a fermentor, where, x_i, resp. s_i, $i = 1, 2$, represent the biomass concentrations, resp. substrate concentrations (after the change of variables), and u is the dilution rate of the continuously operated bioreactor. The index 1, resp. 2 is for the acidogenesis reaction, resp. methanization reaction. The constants s_{in}^1 and s_{in}^2 are positive and denote the two input substrates concentration (after the change of variables).

Following [5], the modeling of biological processes leads to the following choice of the growth rate functions. Both kinetics $\mu_1(\cdot)$ and $\mu_2(\cdot)$ are as follows [13, 16]:

- The growth function $\mu_1(\cdot)$ is of *Monod type*, that is:

$$\mu_1(s_1) = \frac{\bar{\mu}_1 s_1}{k + s_1}, \tag{2.2}$$

  where $\bar{\mu}_1 > 0$ and $k > 0$.

- The growth function $\mu_2(\cdot)$ is of *Haldane type*, that is:

$$\mu_2(s_2) = \frac{\bar{\mu}_2 s_2}{s_2 + k' + \frac{s_2^2}{k''}}, \tag{2.3}$$

  where $\bar{\mu}_2 > 0$, $k' > 0$, and $k'' > 0$. Note that $\mu_2(\cdot)$ has a unique maximum at the point $s_{max} := \sqrt{k'k''}$.

Remark 2.1. *In the model* (1.1)*, proposed in* [5]*, the growth functions $\tilde{\mu}_1(\cdot)$ and $\tilde{\mu}_2(\cdot)$ are of Monod and Haldane type respectively. After the change of variable (indicated in Table 2 of the Appendix in Section 7) for obtaining* (2.1) *from* (1.1)*, it is straightforward to check that the new functions $\mu_1(\cdot)$ and $\mu_2(\cdot)$ are also Monod and Haldane (as it is written above). For this reason, in Table 3 (Appendix in Section 7) we present the parameters of the Monod and Haldane functions $\mu_1(\cdot)$ and $\mu_2(\cdot)$, considering the values obtained experimentally in* [5] *for functions $\tilde{\mu}_1(\cdot)$ and $\tilde{\mu}_2(\cdot)$ in* (1.1)*, after the change of variable. This procedure is explained in the Appendix (Section 7).*

The main feature of an anaerobic fermentor modeled by (2.1) is to transform organic material (the substrates) into biogas (methane). We are interested in studying operation modes of the fermentor for which the production of biogas over a given time period is maximal. In such process, the quantity of biogas over $[0, T]$ is proportional to the quantity

$$\int_0^T \mu_2(s_2(t))x_2(t)\ \mathrm{d}t. \tag{2.4}$$

In order to maximize (2.4) with respect to the dilution rate $u(\cdot)$, a first approach is to study this maximization problem at steady state *i.e.* supposing that the dilution rate u is constant. This amounts to consider the optimization problem

$$\max_{u\in[0,u_{max}]} \mu_2(\bar{s}_2^u)\bar{x}_2^u, \tag{2.5}$$

where $(\bar{x}_1^u, \bar{s}_1^u, \bar{x}_2^u, \bar{s}_2^u)$ is a steady state of (2.1) parametrized by the constant dilution rate u. Here, $u_{max} > 0$ is the maximum value for the dilution rate (it depends on the characteristics of the fermentor). Since this static optimization problem problem was recently studied in [1], we shall only recall one optimality result that will be useful to state the optimal control problem.

Proposition 2.1. *Let* $\tilde{s}_{in}^2 := \min(s_{max}, s_{in}^2)$. *If the parameters* s_{in}^1 *and* s_{in}^2 *satisfy the inequality*

$$s_{in}^1 \geq \mu_1^{-1}(\mu_2(\tilde{s}_{in}^2)), \tag{2.6}$$

then (2.5) *admits an unique optimal solution* $(\bar{x}_1, \bar{s}_1, \bar{x}_2, \bar{s}_2)$ *(steady state of* (2.1)*) such that* $\bar{x}_1 > 0$ *and* $\bar{x}_2 > 0$.

Therefore, if (2.6) holds true, the point that maximizes the static biogas production (problem (2.5)) is such that both species x_i, $i = 1, 2$ coexist at steady state[2]. Moreover, this solution can be written

$$(\bar{x}_1, \bar{s}_1, \bar{x}_2, \bar{s}_2) = \left(\frac{s_{in}^1 - \bar{s}_1}{\alpha}, \bar{s}_1, \frac{s_{in}^1 + s_{in}^2 - \bar{s}_1 - \bar{s}_2}{\alpha}, \bar{s}_2 \right),$$

and it is locally asymptotically stable (see [4, 1]). Hereafter we denote by $\bar{u}$ the corresponding optimal value of the dilution rate.

Remark 2.2. *The complete discussion of the optimization problem* (2.5) *can be found in* [1]. *From a practical point of view, experimental values in* [5] *(see Table 3) indicate that* (2.6) *holds true implying that both species* x_i, $i = 1, 2$ *are present at the optimal equilibrium (see also* [17, 18, 19]*). However, recent results in* [1] *show that other equilibria (such as when the first species* x_1 *is washed-out) could be obtained, but we will restrict our attention in this paper to the case where* (2.6) *holds true which seems to be the case mostly encountered in practice, when* s_{in}^2 *is not too high.*

In the rest of the paper, we consider that the fermentor is operated as in [5] which provides an optimum of problem (2.5) with co-existence of both species. Hence, the optimal solution of (2.5) is supposed to satisfy:

$$\bar{x}_1 > 0 \quad \text{and} \quad \bar{x}_2 > 0.$$

2.2 Statement of the optimal control problem

Before stating the optimal control problem, we recall the following standard attractivity property for system (2.1). When $\alpha = 1$, the set

$$\mathcal{V} := \{(x_1, s_1, x_2, s_2) \in \mathbb{R}_+ \times [0, s_{in}^1] \times \mathbb{R}_+ \times [0, s_{in}^2] \; ; \; x_1 + s_1 = s_{in}^1 \;\text{ and }\; s_1 + x_2 + s_2 = s_{in}^1 + s_{in}^2\},$$

is an invariant and attractive manifold for (2.1). Therefore, trajectories of (2.1) converge asymptotically to this set. In the rest of the paper, we suppose[3] that

$$\alpha = 1,$$

and we only consider initial conditions in the set $\mathcal{V}$. Hence, one has:

$$x_1 = s_{in} - s_1 \quad \text{and} \quad x_2 = s_{in}^1 + s_{in}^2 - s_1 - s_2,$$

thus system (2.1) can be gathered into a two-dimensional affine system as follows:

$$\left\{ \begin{array}{ll} \dot{s}_1 & = (-\mu_1(s_1) + u)(s_{in}^1 - s_1), \\ \dot{s}_2 & = (-\mu_2(s_2) + u)(s_{in}^2 - s_2) + (\mu_1(s_1) - \mu_2(s_2))(s_{in}^1 - s_1), \end{array} \right. \tag{2.7}$$

where $u(\cdot)$ is the control variable which plays the role of the dilution rate. The admissible control set $\mathcal{U}$ is then defined as

$$\mathcal{U} := \{u : [0, +\infty) \to [0, u_{max}] \; ; \; u(\cdot) \text{ meas.}\}.$$

Initial conditions for (2.7) will be taken within the open bounded domain $\mathcal{D}$ defined by:

$$\mathcal{D} := \{s = (s_1, s_2) \in (0, s_{in}^1) \times \mathbb{R}_+^* \; ; \; s_2 < s_{in}^1 + s_{in}^2 - s_1\},$$

[2] Usually, such an equilibrium maximizing the production of biogas at steady state is called *nominal operating point* [17, 18, 19].

[3] When $\alpha < 1$, one can show that the set $\mathcal{V}$ is attractive provided that the constant dilution rate is large enough implying the wash-out of the bacteria. In general, the attractivity property no longer holds when $\alpha < 1$ so that the reduction of (2.1) into (2.7) is not possible, and the problem is more delicate in this case. A thorough study of the control of the chemostat system (*i.e.* the restriction of (2.1) to (x_1, s_1)) including a retention of biomass parameter can be found in [2].

that is invariant by (2.7). In order to introduce properly the target point, it is convenient to write (2.7) as a two dimensional affine system with one input and a drift:

$$\dot{s} = f(s) + ug(s), \tag{2.8}$$

where $s = (s_1, s_2)$ and $f, g : \mathbb{R}^2 \to \mathbb{R}^2$ are the two vector fields defined by

$$f(s) = \begin{bmatrix} -\mu_1(s_1)(s_{in}^1 - s_1) \\ -\mu_2(s_2)(s_{in}^2 - s_2) + (\mu_1(s_1) - \mu_2(s_2))(s_{in}^1 - s_1) \end{bmatrix} \quad \text{and} \quad g(s) = \begin{bmatrix} s_{in}^1 - s_1 \\ s_{in}^2 - s_2 \end{bmatrix}.$$

The *collinearity curve* Δ_0 is then defined as the set of points of $\mathcal{D}$ where f and g are collinear *i.e.*

$$\Delta_0 := \{s \in \mathcal{D} \; ; \; \det(f(s), g(s)) = 0\}. \tag{2.9}$$

This set is essential in particular for studying controllability issues of (2.7). A straightforward computation gives

$$\det(f(s), g(s)) = (s_{in}^1 - s_1)(s_{in}^1 + s_{in}^2 - s_1 - s_2)(\mu_2(s_2) - \mu_1(s_1)),$$

and since initial conditions are in $\mathcal{D}$, one has $s_1 < s_{in}^1$ and $s_{in}^1 + s_{in}^2 - s_1 - s_2 > 0$. Therefore, Δ_0 can be equivalently written:

$$\Delta_0 := \{s = (s_1, s_2) \in \mathcal{D} \; ; \; \mu_1(s_1) = \mu_2(s_2)\}. \tag{2.10}$$

As both functions $\mu_1(\cdot)$ and $\mu_2(\cdot)$ are continuous and strictly increasing in a neighborhood of zero, one can check that Δ_0 is non-empty (the curve Δ_0 is depicted on Figure 1).

In this paper, our aim is to consider the problem of steering (2.7) in minimal time to the target point maximizing the biogas production at steady state. As we supposed that (s_{in}^1, s_{in}^2) satisfies the assumptions of Proposition 2.1, one has that the unique optimal solution $(\bar{x}_1, \bar{s}_1, \bar{x}_2, \bar{s}_2)$ (steady state of (2.1)) of the optimization problem (2.5) is such that $\bar{x}_1 > 0$ and $\bar{x}_2 > 0$. Therefore, the optimal steady state $(\bar{s}_1, \bar{s}_2)$ of (2.7), that is our target, satisfies:

$$\mu_1(\bar{s}_1) = \mu_2(\bar{s}_2),$$

since one should have $\mu_i(\bar{s}_i) = \bar{u}$. This implies that

$$\bar{s} := (\bar{s}_1, \bar{s}_2) \in \Delta_0. \tag{2.11}$$

Hence, the target point $\bar{s}$ belongs to the collinearity set Δ_0. The minimum time control problem can be then stated as follows : given $\bar{s} \in \Delta_0$, we consider the optimal problem:

$$v(s^0) := \inf_{u \in \mathcal{U}} T_u \quad \text{s.t.} \quad s_u(T_u) = \bar{s}, \tag{2.12}$$

where $s_u(\cdot)$ is the unique solution of (2.7) associated to the control u and starting from a given initial condition $s^0 := (s_1^0, s_2^0) \in \mathcal{D}$. Here, $s^0 \in \mathcal{D} \mapsto v(s^0) \in [0, +\infty]$ is the value function, and our aim is to obtain an optimal control for (2.12) in feedback form. At this step, it is worth to mention that we propose to solve (2.12) for any given value of the target point $\bar{s} \in \Delta_0$ (not only the optimal steady state point). In fact, due to uncertainties that can affect the real process, the real value of $\bar{s}$ may not be known exactly, and thus it is important to find an optimal synthesis of the problem for any given value of $\bar{s} \in \Delta_0$.

Note that if the target point can be reached from a given initial condition $s^0 \in \mathcal{D}$, then the existence of an optimal control for (2.12) is standard using Filippov's Theorem (see *e.g.* [11]).

3 Optimality conditions and geometric properties of the system

3.1 Pontryagin Maximum Principle

In this section, we apply the Pontryagin Maximum Principle (PMP) on (2.12) in order to derive necessary optimality conditions on an optimal control u. To this end, let $H : \mathbb{R}^2 \times \mathbb{R}^2 \times \mathbb{R} \times \mathbb{R}$ be the Hamiltonian associated to (2.12):

$$H = H(s, \lambda, \lambda_0, u) := \lambda \cdot f(s) + u\lambda \cdot g(s) + \lambda_0, \tag{3.1}$$

where $a \cdot b$ denotes the scalar product in $\mathbb{R}^2$, that is:

$$H = -\lambda_1\mu_1(s_1)(s_{in}^1 - s_1) + \lambda_2[-\mu_2(s_2)(s_{in}^2 - s_2) + (\mu_1(s_1) - \mu_2(s_2))(s_{in}^1 - s_1)] \\ + u[\lambda_1(s_{in}^1 - s_1) + \lambda_2(s_{in}^2 - s_2)] + \lambda_0.$$

Now, let s^0 be a given initial condition in $\mathcal{D}$ and $u \in \mathcal{U}$ an optimal control of (2.12) steering (2.7) in time T_u from s^0 to $\bar{s}$. Then, the following conditions hold true:

- There exists $\lambda_0 \leq 0$ and an absolutely continuous function $\lambda : [0, T_u] \to \mathbb{R}^2$ called *adjoint vector* satisfying the adjoint equation $\dot{\lambda} = -\frac{\partial H}{\partial s}(s(t), \lambda(t), \lambda_0, u(t))$ for a.e. $t \in [0, T_u]$, that is:

$$\begin{cases} \dot{\lambda}_1 &= \lambda_1[\mu_1'(s_1)(s_{in}^1 - s_1) - \mu_1(s_1) + u] - \lambda_2[\mu_1'(s_1)(s_{in}^1 - s_1) - \mu_1(s_1) + \mu_2(s_2)], \\ \dot{\lambda}_2 &= \lambda_2[\mu_2'(s_2)(s_{in}^2 - s_2) - \mu_2(s_2) + u + \mu_2'(s_2)(s_{in}^1 - s_1)]. \end{cases} \tag{3.2}$$

- The vector $(\lambda_1(\cdot), \lambda_2(\cdot), \lambda_0)$ is non-zero.
- We have the maximization condition : for a.e. $t \in [0, T_u]$,

$$u(t) \in \arg \max_{\omega \in [0, u_{max}]} H(s(t), \lambda(t), \lambda_0, \omega). \tag{3.3}$$

We call *extremal trajectory* a quadruple $(s(\cdot), \lambda(\cdot), \lambda_0, u(\cdot))$ satisfying (2.7)-(3.2)-(3.3). When $\lambda_0 = 0$, we say that the extremal is *abnormal* whereas if $\lambda_0 < 0$, then we say that the extremal is *normal*. In the latter, we can assume that $\lambda_0 = -1$ and therefore, by homogeneity, we write $(s(\cdot), \lambda(\cdot), u(\cdot))$ in place of $(s(\cdot), \lambda(\cdot), \lambda_0, u(\cdot))$. Observe that the Hamiltonian is conserved along any extremal trajectory. In addition, one has $H = 0$ along any extremal trajectory since the terminal time is free.

It is convenient to introduce the *switching function* $\phi(t) := \lambda(t) \cdot g(s(t))$ (the term multiplying the control u in the Hamiltoninan H defined in (3.1)) that provides the control law. From (3.3), one deduces that:

$$\begin{cases} \phi(t) > 0 &\Rightarrow \quad u(t) = u_{max}, \\ \phi(t) < 0 &\Rightarrow \quad u(t) = 0, \\ \phi(t) = 0 &\Rightarrow \quad u(t) \in [0, u_{max}]. \end{cases}$$

We call *switching time* any time $t_c \in (0, T_u)$ such that the optimal control $u(\cdot)$ is non-constant in any neighborhood of t_c, which implies $\phi(t_c) = 0$. We then say that the corresponding trajectory has a *switching point*. A *singular arc* is a time interval $[t_1, t_2] \subset [0, T_u]$ where the switching function satisfies $\phi(t) = 0$ for any time $t \in [t_1, t_2]$. In order to study properties of singular arcs, we introduce the *singular locus* Δ_{SA} defined as :

$$\Delta_{SA} := \{ s = (s_1, s_2) \in \mathcal{D} \, ; \det(g(s), [f, g](s)) = 0 \, \},$$

where $[f, g](s)$ denotes the Lie bracket[4] associated to the vector fields f and g. Following for instance [9], it is well-known that any singular arc is such that the associated trajectory belongs to the singular locus Δ_{SA}. Since one has

$$\det(g(s), [f, g](s)) = (s_{in}^1 - s_1)(s_{in}^1 + s_{in}^2 - s_1 - s_2)[\mu_2'(s_2)(s_{in}^2 - s_2) - \mu_1'(s_1)(s_{in}^1 - s_1)],$$

we deduce that Δ_{SA} can be expressed as

$$\Delta_{SA} = \{ s = (s_1, s_2) \in \mathcal{D} \, ; \; \mu_2'(s_2)(s_{in}^2 - s_2) - \mu_1'(s_1)(s_{in}^1 - s_1) = 0 \, \}. \tag{3.4}$$

Next, the function $\theta : \mathcal{D} \backslash \Delta_0 \to \mathbb{R}$ defined by

$$\theta(s) := \frac{\mu_1'(s_1)(s_{in}^1 - s_1) - \mu_2'(s_2)(s_{in}^2 - s_2)}{\mu_1(s_1) - \mu_2(s_2)} = \frac{\det(g(s), [f, g](s))}{\det(f(s), g(s))}, \tag{3.5}$$

will be crucial to exclude non-optimal extremal trajectories.

[4]The Lie bracket of two smooth vector fields $f, g : \mathbb{R}^2 \to \mathbb{R}^2$ is the vector field $[f, g] : \mathbb{R}^2 \to \mathbb{R}^2$ defined by $[f, g](s) := Dg(s)f(s) - Df(s)g(s)$, $s \in \mathbb{R}^2$.

Proposition 3.1. *Let $(s(\cdot), \lambda(\cdot), u(\cdot))$ be a normal extremal trajectory defined over $[0, T_u]$ with $T_u \geq 0$. Then, there exists a function $\gamma : (\mathcal{D}\backslash\Delta_0) \times (0, T_u) \to \mathbb{R}$ such that:*
(i) For any time $t \in (0, T_u)$ such that $s(t) \notin \Delta_0$ one has:

$$\dot{\phi}(t) = \gamma(s(t), t)\phi(t) - \theta(s(t)). \tag{3.6}$$

(ii) If the trajectory has a switching point at a time t_c such that $\theta(s(t_c)) > 0$, resp. $\theta(s(t_c)) < 0$, then it is a switching time from $u = u_{max}$ to $u = 0$, resp. from $u = 0$ to $u = u_{max}$.

Proof. When $s \in \mathcal{D}\backslash\Delta_0$, one has $\text{span}\{f(s), g(s)\} = \mathbb{R}^2$, therefore there exists $\alpha(s) \in \mathbb{R}$ and $\beta(s) \in \mathbb{R}$ such that

$$[f, g](s) = \alpha(s)f(s) + \beta(s)g(s).$$

From this equality, we deduce that $\alpha(s) = -\frac{\det(g(s),[f,g](s))}{\det(f(s),g(s))} = -\theta(s)$, where function $\theta(\cdot)$ is defined in (3.5). Now, let us consider a normal trajectory $(s(\cdot), \lambda(\cdot), u(\cdot))$. If we differentiate ϕ with respect to t, we find that:

$$\dot{\phi}(t) = \lambda(t) \cdot [f, g](s(t)) = \alpha(s(t))\lambda(t) \cdot f(s(t)) + \beta(s(t))\phi(t) = \alpha(s(t)) + \phi(t)(\beta(s(t)) - \alpha(s(t))u(t)),$$

supposing that $s(t) \notin \Delta_0$ (the last equality above follows using that $H = \lambda(t) \cdot f(s(t)) + u(t)\phi(t) - 1 = 0$ for $t \in [0, T_u]$). Thus, if we set $\gamma(s, t) := \beta(s) - \alpha(s)u(t)$ for $(s, t) \in (\mathcal{D}\backslash\Delta_0) \times (0, T_u)$, we find (3.6) which proves (i). To prove (ii), suppose that t_c is a switching time such that $\theta(s(t_c)) > 0$. We then deduce from (3.6) that $\dot{\phi}(t_c) < 0$ implying that t_c is a switching time from $u = u_{max}$ to $u = 0$. The proof is similar if $\theta(s(t_c)) < 0$. □

Next, let us introduce the two subsets of $\mathcal{D}$, $\Delta_0^{\pm}$, defined by:

$$\Delta_0^+ := \{s \in \mathcal{D} \,;\, \det(f(s), g(s)) > 0\} \quad \text{and} \quad \Delta_0^- := \{s \in \mathcal{D} \,;\, \det(f(s), g(s)) < 0\}.$$

The next Lemma is straightforward from the adjoint equation (3.2).

Lemma 3.1. *For any extremal trajectory, the corresponding adjoint vector $\lambda(\cdot) = (\lambda_1(\cdot), \lambda_2(\cdot))$ is such that $\lambda_2 \equiv 0$ or λ_2 is always of constant sign.*

The next proposition allows us to exclude extremal trajectories crossing the set Δ_0 and with at least one switching point in each component Δ_0^+ and Δ_0^-.

Proposition 3.2. *A normal extremal trajectory $(s(\cdot), \lambda(\cdot), u(\cdot))$ cannot have two switching points $t_1 < t_2$ such that $s(t_1) \in \Delta_0^{\pm}$ and $s(t_2) \in \Delta_0^{\mp}$.*

Proof. From Lemma 3.1, either $\lambda_2 \equiv 0$ or λ_2 is always non-zero. Suppose that $\lambda_2 \equiv 0$. Then, λ_1 cannot vanish. Otherwise, there would exist a time t such that $\lambda_1(t) = \lambda_2(t) = 0$. By Cauchy-Lipschitz's Theorem, we would then also have $\lambda_1 \equiv 0$. Since $H = 0$, we deduce that $\lambda_0 = 0$ which contradicts the PMP. Hence, λ_1 is always non-zero implying that $\phi = \lambda_1(s_{in}^1 - s_1)$ is of constant sign, which is also a contradiction because $(s(\cdot), \lambda(\cdot), u(\cdot))$ has a switching point. We deduce that $\lambda_2(\cdot)$ is always non-zero.

Without any loss of generality, we suppose that the two switching times occur in Δ_0^+ at time t_1 and in Δ_0^- at time $t_2 > t_1$. Using that $\phi(t_i) = 0$ and $H = 0$, one obtains:

$$\lambda_2(t_1)(s_{in}^1 + s_{in}^2 - s_1(t_1) - s_2(t_1))(\mu_1(s(t_1)) - \mu_2(s(t_1))) = 1,$$

and

$$\lambda_2(t_2)(s_{in}^1 + s_{in}^2 - s_1(t_2) - s_2(t_2))(\mu_1(s(t_2)) - \mu_2(s(t_2))) = 1.$$

Now, λ_2 is of constant sign (positive for instance) and $s_{in}^1 + s_{in}^2 - s_1(t_i) - s_2(t_i) > 0$ for $i = 1, 2$ whereas $\mu_1(s(t_1)) - \mu_2(s(t_1)) > 0$ and $\mu_1(s(t_2)) - \mu_2(s(t_2)) < 0$, thus we have a contradiction. This ends the proof. □

Remark 3.1. *The above result give us some information related switching points of a normal extremal trajectories $(s(\cdot), \lambda(\cdot), u(\cdot))$. Recall that if $(s(\cdot), \lambda(\cdot), u(\cdot))$ is an abnormal extremal trajectory, one can have switching points on the curve Δ_0 only (see e.g. [9]).*

It follows that any normal extremal trajectory can have switching points either in Δ_0^+ or in Δ_0^- (but not both in the two components). By the previous proposition, we also obtain that given a normal extremal trajectory $(s(\cdot), \lambda(\cdot), u(\cdot))$, then:

- If $\lambda_2(t) = 0$ for any time $t \in [0, T_u]$, then the control is constant over $[0, T_u]$ (equal to 0 or u_{max}).
- If $\lambda_2(t) > 0$ for any time $t \in [0, T_u]$, then switching points in $\mathcal{D}$ necessarily occur in Δ_0^-.
- If $\lambda_2(t) < 0$ for any time $t \in [0, T_u]$, then switching points in $\mathcal{D}$ necessarily occur in Δ_0^+.

3.2 Geometric properties of the system

Before going further into the determination of optimal controls, we provide a more detailed insight into the geometrical characteristics of system (2.7).

3.2.1 Collinearity set

First, we give some geometrical properties of the collinearity curve Δ_0. In the rest of the paper, we suppose that

$$\bar{\mu}_1 > \mu_2(s_{max}), \tag{3.7}$$

where $\bar{\mu}_1$ is the maximal (asymptotic) value of function $\mu_1(\cdot)$ defined in (2.2), that is, $\mu_1(s_1) < \bar{\mu}_1$ for all $s_1 \geq 0$, and s_{max} is the point where function $\mu_2(\cdot)$, defined in (2.3), attains its maximum, that is $s_{max} := \sqrt{k'k''}$. In view of the numerical values of parameters in the definitions of $\mu_1(\cdot)$ and $\mu_2(\cdot)$ (see Table 3), one can check that condition (3.7) holds true. This property allows to give an analytical description of set Δ_0 defined in (2.9) and (2.10). Indeed, one has

$$(s_1, s_2) \in \Delta_0 \iff \mu_1(s_1) = \mu_2(s_2) \iff s_1 = \delta_0(s_2) := (\mu_1)^{-1}(\mu_2(s_2)),$$

where δ_0 is the real-valued function defined over $\mathbb{R}_+$ by:

$$\delta_0(s_2) = \frac{k_1\mu_2(s_2)}{\bar{\mu}_1 - \mu_2(s_2)}.$$

Thanks to (3.7), one has $\bar{\mu}_1 > \mu_2(s_2)$ for any $s_2 \geq 0$, thus the previous expression of δ_0 is well defined. By differentiating δ_0 with respect to s_2 one obtains $\delta_0'(s_2) = \frac{k_1\bar{\mu}_1\mu_2'(s_2)}{(\bar{\mu}_1 - \mu_2(s_2))^2}$, therefore δ_0 is increasing over $[0, s_{max}]$ and decreasing over $[s_{max}, +\infty)$. In our case, that is, considering the experimental values obtained in [5] (see Table 3), one has $\tilde{s}_{in}^2 = s_{max}$, thus (2.6) implies that $\mu_1(s_{in}^1) \geq \mu_2(s_{max})$. As a consequence, one has

$$\delta_0(s_2) \in [0, s_{in}^1],$$

for any $s_2 \in \mathbb{R}_+$ because $\mu_1(s_{in}^1) \geq \mu_2(s_{max}) \geq \mu_2(s_2)$. The graph of Δ_0 is depicted on Figure 1. As a consequence, we obtain that $\Delta_0^{\pm}$ are such that:

$$\Delta_0^+ = \{s = (s_1, s_2) \in \mathcal{D}\ ;\ s_1 < \delta_0(s_2)\} \quad \text{and} \quad \Delta_0^- = \{s = (s_1, s_2) \in \mathcal{D}\ ;\ s_1 > \delta_0(s_2)\}.$$

The following property is straightforward and it is essential to analyze the behavior of extremal trajectories (see Figure 1).

Property 3.1. *One has*

$$\begin{aligned} \det(f(s), f(s) + g(s)) > 0 &\iff \mu_1(s_1) < \mu_2(s_2) \iff (s_1, s_2) \in \Delta_0^+, \\ \det(f(s), f(s) + g(s)) < 0 &\iff \mu_1(s_1) > \mu_2(s_2) \iff (s_1, s_2) \in \Delta_0^-. \end{aligned}$$

3.2.2 Singular locus

As for Δ_0, we provide an analytic description of the singular locus Δ_{SA} defined in (3.4). First, we define two functions $s_i \mapsto \nu_i(s_i)$ $(i = 1, 2)$ by

$$\nu_i(s_i) := \mu_i'(s_i)(s_{in}^i - s_i) \qquad i = 1, 2.$$

From (3.4) notice that

$$(s_1, s_2) \in \Delta_{SA} \iff \nu_1(s_1) = \nu_2(s_2) \quad \text{and} \quad (s_1, s_2) \in \mathcal{D}.$$

On the other hand, from the definitions of $\mu_1(\cdot)$ and $\mu_2(\cdot)$ in (2.2) and (2.3) respectively, it is straightforward to check that $\nu_1'(s_1) > 0$ for all $s_1 > 0$ and $\nu_2'(s_2) > 0$ for all $s_2 \in [0, \tilde{s}_{in}^2)$, where $\tilde{s}_{in}^2 := \min(s_{max}, s_{in}^2)$. Therefore, functions $\nu_i(\cdot)$ are increasing in the corresponding intervals. In the following, we will assume that the equation $\nu_1(s_1) = \nu_2(s_2)$ does not admit a solution $(s_1, s_2) \in \mathcal{D}$ such that $s_2 \in (s_{max}, s_{in}^1 + s_{in}^2 - s_1)$. Assuming that the equation $\nu_1(s_1) = \nu_2(s_2)$ does not admit a solution $(s_1, s_2) \in \mathcal{D}$ such that $s_2 \in (s_{max}, s_{in}^1 + s_{in}^2 - s_1)$, allows to conclude that the singular locus Δ_{SA} is composed by only one connected component in $\mathcal{D}$.

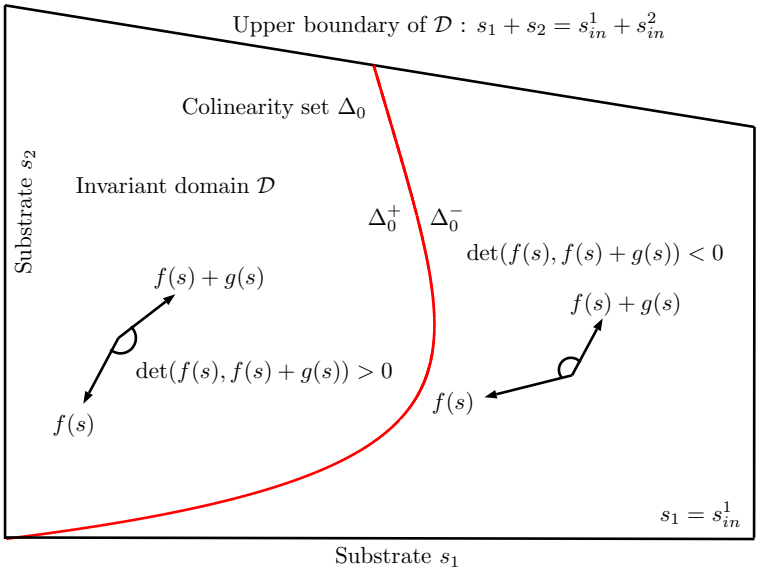

Figure 1: Plot of Δ_0 ; the curve Δ_0 partitions $\mathcal{D}$ into the two subsets $\Delta_0^{\pm}$. In Δ_0^+, resp. Δ_0^-, one has $\det(f(s), f(s)+g(s)) > 0$, resp. $\det(f(s), f(s)+g(s)) < 0$.

Property 3.2. *A sufficient condition ensuring that Δ_{SA} is simply connected is to have*

$$\mu_1'(s_{in}^1) + \mu_2'(s_2^\dagger) > 0, \tag{3.8}$$

where $s_2^\dagger := \min(s_{in}^1 + s_{in}^2, s^{**})$ and s^{**} is the unique point where $\mu_2''(\cdot)$ vanishes.

Proof. Indeed, (3.8) implies that

$$\mu_1'(s_1) + \mu_2'(s_2) > 0,$$

for all $s_1 \in (0, s_{in}^1)$ and $s_2 \in (s_{max}, s_{in}^1 + s_{in}^2 - s_1)$ since μ_2' is decreasing over $[s_{max}, s^{**}]$ and increasing over $[s^{**}, +\infty)$. Now, take $(s_1, s_2) \in \mathcal{D}$ and suppose that $\nu_1(s_1) = \nu_2(s_2)$. If $s_2 \leq s_{in}^2$, then one must have $\mu'(s_2) > 0$ and thus $s_2 \leq s_{max}$. Now, suppose that $s_2 > s_{in}^2$. As $\nu_1(s_1) = \nu_2(s_2)$, we necessarily have $\mu'(s_2) < 0$. It follows that

$$\mu_1'(s_1)(s_{in}^1 - s_1) = \mu_2'(s_2)(s_{in}^2 - s_2) < -\mu_2'(s_2)(s_{in}^1 - s_1),$$

using that $s_{in}^2 - s_2 > -(s_{in}^1 - s_1)$. We thus obtain a contradiction Therefore, the equation $\nu_1(s_1) = \nu_2(s_2)$ cannot have a solution (s_1, s_2) such that $s_2 \in (s_{max}, s_{in}^1 + s_{in}^2 - s_1)$ as was to be proved. □

In our case, that is, considering the experimental values obtained in [5] (see Table 3), we have $s_2^\dagger = s^{**} \simeq 34.0275$, and $\mu_1'(s_{in}^1) + \mu_2'(s_2^\dagger) \simeq 0.0264$. Moreover, if $(s_1, s_2) \in \Delta_{SA}$, then $s_2 < s_{max}$. Now, from (3.4), we obtain

$$(s_1, s_2) \in \Delta_{SA} \iff (s_1, s_2) \in \mathcal{D} \quad \text{and} \quad s_1 = \delta_{SA}(s_2) := (\nu_1)^{-1}(\nu_2(s_2)), \tag{3.9}$$

where $(\nu_1)^{-1}$ is well defined because $\nu_1(\cdot)$ is increasing in $[0, +\infty)$ and $\nu_2(s_2) > 0$ for all $s_2 \in (0, s_{max})$. A direct computation gives

$$\delta_{SA}(s_2) = k\frac{-\bar{\mu}_1 - 2\nu_2(s_2) + \sqrt{\bar{\mu}_1^2 + 4\bar{\mu}_1\nu_2(s_2) + 4\frac{s_{in}^1\bar{\mu}_1}{k}\nu_2(s_2)}}{2\nu_2(s_2)}.$$

The graph of Δ_{SA} is depicted on Figure 3. Using the numerical values indicated on Table 3 (Section 7), one can check that the singular locus passes through the points $(s_{in}^1, s_{max}) = (s_{in}^1, \sqrt{k'k''}) \simeq (10, 17.63)$ and $(0, \delta_{SA}^{-1}(0)) \simeq (0, 3.15)$ whereas the graph of Δ_0 passes through $(0, 0)$ and intersects the upper boundary of $\mathcal{D}$. It is then to expect that the intersection of Δ_0 and Δ_{SA} will be non-empty.

It appears that the non-vacuity of $\Delta_0 \cap \Delta_{SA}$ is crucial in the forthcoming study (see *e.g.* [3]). For this reason, we introduce the following definition.

Definition 3.1. *We say that a point $s^\star \in \mathcal{D}$ is a steady state singular point if $s^\star \in \Delta_0 \cap \Delta_{SA}$ and $g(s^\star) \neq 0$, where $g(\cdot)$ is the drift function in* (2.8).

In our setting, we have that $g(\cdot)$ is non-zero in $\mathcal{D}$. Moreover, with the experimental values obtained in [5] (see Table 3 in Section 7), we can check numerically that there exists exactly one *steady state singular point*:

$$s^\star := (5.08, 8.73),$$

located at the intersection of Δ_0 and Δ_{SA}. In the sequel, we shall therefore suppose that the intersection of Δ_0 and Δ_{SA} in $\mathcal{D}$ is reduced to exactly one point. Recall from [3] the two following properties (see also [9]):

- Any steady state singular point is an equilibrium of (2.7) restricted to the set Δ_{SA}.
- The dynamics (2.7) is collinear to the tangent vector to the graph of Δ_0 at some point $s \in \Delta_0$ if and only if s is a steady state singular point (see Figure 3).

We continue the study of the singular locus, computing the *singular control* $t \mapsto u_s(t)$ that is defined for each time t as the control u for which the corresponding trajectory $s(t)$ is such that $s(t) \in \Delta_{SA}$. It is obtained by differentiating ϕ twice with respect to the time t. We thus obtain

$$\ddot{\phi}(t) = a(s(t)) + u_s(t)b(s(t)),$$

where $s \mapsto a(s)$ and $s \mapsto b(s)$ are defined respectively by:

$$\begin{aligned} a(s) :=& [\mu_2(s_2)(s_{in}^1 + s_{in}^2 - s_1 - s_2) - \mu_1(s_1)(s_{in}^1 - s_1)][\mu_2''(s_2)(s_{in}^2 - s_2) - \mu_2'(s_2)] \\ & - \mu_1(s_1)(s_{in}^1 - s_1)[\mu_1''(s_1)(s_{in}^1 - s_1) - \mu_1'(s_1)], \quad s \in \mathcal{D} \end{aligned}$$

and

$$b(s) := \mu_1''(s_1)(s_{in}^1 - s_1)^2 - \mu_2''(s_2)(s_{in}^2 - s_2)^2, \quad s \in \mathcal{D}. \tag{3.10}$$

Hence, we deduce that along a singular trajectory $t \mapsto s(t)$, one has:

$$u_s(t) := -\frac{a(s(t))}{b(s(t))}. \tag{3.11}$$

The plot of the singular control u_s is depicted on Figure 4. In (3.11), the control u_s can be expressed as a function of the variable s_2 (*i.e.* in feedback form) using that along the singular arc one has $s_1 = \delta_{SA}(s_2)$. With a slight abuse of notation, we denote by $s_2 \mapsto u_s(s_2)$ the singular control defined by (3.11) where s_1 has been replaced by $\delta_{SA}(s_2)$. Hence, we find that

$$u_s(s_2) = -\frac{a(\delta_{SA}(s_2), s_2)}{b(\delta_{SA}(s_2), s_2)}, \quad s_2 \in [0, s_{max}]. \tag{3.12}$$

In the sequel, we shall suppose that u_{max} is large enough to ensure the admissibility of the singular arc, that is, we assume that u_{max} satisfies:

$$\forall s_2 \in [0, s_2^{max}], \quad u_s(s_2) \in [0, u_{max}]. \tag{3.13}$$

Remark 3.2. *In the case where $u_s(\cdot)$ takes larger values than u_{max}, then a saturation phenomenon may occur leading to the existence of an additional switching curve emanating from the singular locus. For simplicity, we assumed in this study that this case does not happen by choosing a sufficiently large value for the maximum dilution rate (this is always possible from a practical point of view).*

In the following lemma, we prove that the unique steady state singular point is is attractive for the dynamics (2.7) restricted to the singular locus Δ_{SA}.

Lemma 3.2. *If $\Delta_0 \cap \Delta_{SA} = \{s^\star\}$, Δ_{SA} is composed only by one connected component in $\mathcal{D}$, and there exists $(s_1, s_2) \in \Delta_{SA}$ with $s_1 \to 0$, then $s^\star = (s_1^\star, s_2^\star)$ is attractive for the dynamics* (2.7) *restricted to the singular locus Δ_{SA}.*

Proof. We will study the sign of $\dot{s}_{1_{|\Delta_{SA}}}$, that is, the derivative of $s_1(\cdot)$ restricted to the singular locus Δ_{SA}. From the expression of the singular control u_s in (3.11), notice that $u_s(s_2 \to \mu_2(s_{max}) < \mu_1(s_{in}^1)$ (see (2.6)) when $\Delta_{SA} \ni (s_1, s_2) \to (s_{in}^1, s_{max})$. Therefore, $\dot{s}_1 < 0$ when $\Delta_{SA} \ni (s_1, s_2) \to (s_{in}^1, s_{max})$ (see the dynamics (2.7)). On the other hand, $\dot{s}_1 > 0$ when $(s_1, s_2) \in \Delta_{SA}$ and $s_1 \to 0$. We conclude then that $\dot{s}_1 > 0$ if $s_1 < s_1^\star$ and $\dot{s}_1 < 0$ if $s_1 > s_1^\star$, proving thus that $s^\star = (s_1^\star, s_2^\star)$ is attractive for the dynamics (2.7) restricted to the singular locus Δ_{SA}. □

We can check numerically the result given by the previous lemma, observing that the steady state singular point $s^\star = (s_1^\star, s_2^\star)$ is attractive for the dynamics (2.7) restricted to the singular locus Δ_{SA} as shows Figure 2.

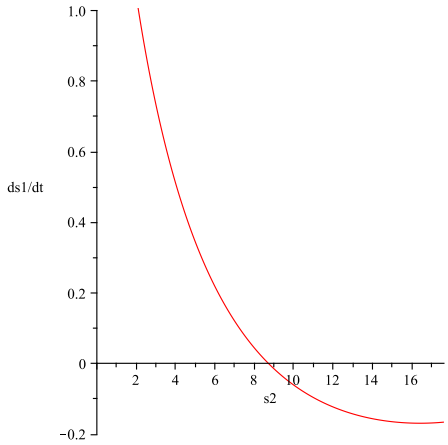

Figure 2: Plot of $\dot{s}_1$ along the singular arc (as a function of s_2 since Δ_{SA} was parametrized as a function of s_2, see (3.9)). The point $s^\star$ is attractive for (2.7) restricted to Δ_{SA} since one has $\dot{s}_1 > 0$ for $s_1 < s_1^\star$, $\dot{s}_1 < 0$ for $s_1 > s_1^\star$, and $\dot{s}_1 = 0$ for $s_1 = s_1^\star$.

Similarly as for Δ_0, and under the assumption that the set Δ_{SA} is composed only by one connected curve in $\mathcal{D}$, we have that Δ_{SA} partitions $\mathcal{D}$ into two connected subsets $\Delta_{SA}^\pm$ (see Figure 3) defined respectively by:

$$\begin{cases} \Delta_{SA}^+ := \{s \in \mathcal{D}\ ;\ \det(g(s), [f,g](s)) > 0\} = \{s = (s_1, s_2) \in \mathcal{D}\ ;\ s_1 > \delta_{SA}(s_2)\}, \\ \Delta_{SA}^- := \{s \in \mathcal{D}\ ;\ \det(g(s), [f,g](s)) < 0\} = \{s = (s_1, s_2) \in \mathcal{D}\ ;\ s_1 < \delta_{SA}(s_2)\}. \end{cases}$$

We can then depict the sign of the function $\theta(s) = \frac{\det(g(s),[f,g](s))}{\det(f(s),g(s))}$ (defined in (3.5)) in each component $\Delta_0^\pm \cap \Delta_{SA}^\pm$, see Figure 3.

Let us finally analyze the local optimality of singular arcs by utilizing the generalized *Legendre-Clebsch* necessary optimality condition [20]. The notation H_u will stand for the derivative of H with respect to u. Recall that if a singular arc is optimal over a time interval $[t_1, t_2]$, then one must have

$$\frac{\partial}{\partial u}\frac{d^2 H_u}{dt^2} \geq 0,$$

along the corresponding singular trajectory (see *e.g.* [9, 20]). Following [20], one has:

$$\frac{\partial}{\partial u}\frac{d^2 H_u}{dt^2}(t) = \langle \lambda(t), [g,[f,g]](s(t)) \rangle\,,$$

where for convenience we wrote $H_u(t)$ in place of $H_u(s(t), \lambda(t), u(t))$. Along a singular trajectory, it can be also verified (see [3]) that the adjoint vector is expressed by

$$\lambda(t) := \frac{g^\perp(s(t))}{\det(f(s(t)), g(s(t)))},$$

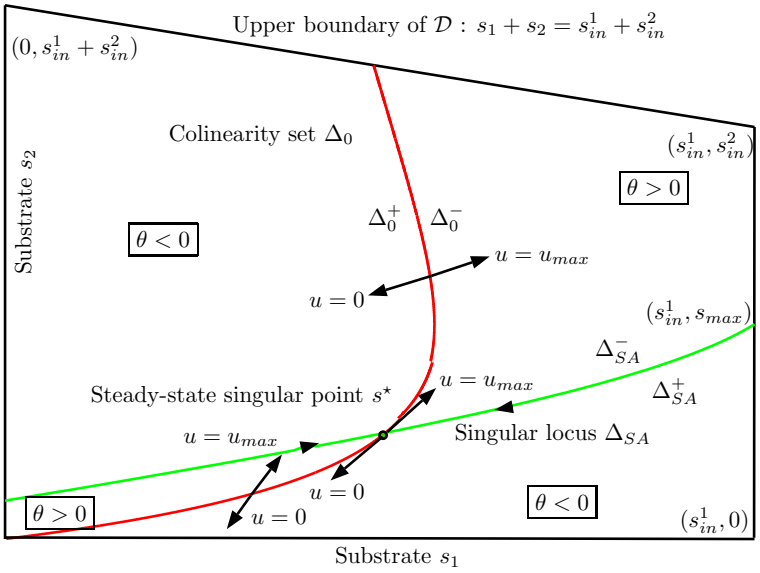

Figure 3: Plot of Δ_0, $\Delta_0^\pm$, Δ_{SA}, $\Delta_{SA}^\pm$, and of the steady state singular point $s^\star \in \Delta_0 \cap \Delta_{SA}$ (that is attractive for (2.7) restricted to Δ_{SA}). The sign of $s \mapsto \theta(s)$ depends on the position of $s \in \Delta_0^\pm \cap \Delta_{SA}^\pm$. We also indicated in the figure the direction of the dynamics (2.7) with $u = u_{max}$ or $u = 0$ on the curve Δ_0.

where $s(\cdot)$ is the corresponding singular trajectory and for $a = (a_1, a_2) \in \mathbb{R}^2$, $a^\perp := (a_2, -a_1)$. A direct computation of $[g, [f, g]]$ then gives:

$$[g,[f,g]](s) = \begin{pmatrix} \mu_1''(s_1)(s_{in}^1 - s_1)^3 - \mu_1'(s_1)(s_{in}^1 - s_1)^2 \\ -\mu_1''(s_1)(s_{in}^1 - s_1)^3 + \mu_2''(s_2)(s_{in}^1 + s_{in}^2 - s_1 - s_2)(s_{in}^2 - s_2)^2 + \mu_1'(s_1)(s_{in}^1 - s_1)^2 \\ -\mu_2'(s_2)(s_{in}^2 - s_2)(s_{in}^1 + s_{in}^2 - s_1 - s_2) \end{pmatrix}.$$

Therefore, we find that along a singular trajectory one has (we removed the time variable below to shorten the notation):

$$\langle \lambda, [g,[f,g]](s) \rangle = \frac{(s_{in}^1 - s_1)(s_{in}^1 + s_{in}^2 - s_1 - s_2)}{\det(f(s), g(s))} [\mu_1''(s_1)(s_{in}^1 - s_1)^2 - \mu_2''(s_2)(s_{in}^2 - s_2)^2].$$

The sign of $\frac{\partial}{\partial u} \frac{d^2 H_u}{dt^2}$ then only depends on the position of the singular arc with respect to Δ_0 (*i.e.* on the sign of $\det(f(s), g(s))$) and on the sign of the mapping $s \mapsto b(s)$ (defined in (3.10)) computed along the singular locus *i.e.* with $s_1 = \delta_{SA}(s_2)$. Using the numerical datas indicated in Table 3, we can check that $s \mapsto b(s)$ is positive along the singular locus (see Figure 4).

Let us now recall the standard definitions of turnpike and anti-turnpike singular arcs for planar affine systems (see [9, 20]).

Definition 3.2. *If a singular arc is locally optimal, then it is called turnpike. When it is not locally optimal, then it is called an anti-turnpike.*

In the case where a singular arc is a turnpike, we say equivalently that it is *time minimizing* (see [9]) whereas for an anti-turnpike, we say that it is *time-maximizing*. Since the quantity $\det(f(s), g(s))$ changes its sign on the curve Δ_0, we obtain the following property for the singular locus.

Proposition 3.3. *The singular locus is time minimizing in Δ_0^+ and it is time maximizing in Δ_0^-.*

Proof. Consider a singular arc over $[t_1, t_2]$. Since $b(\cdot)$ is non-negative on the singular locus, we find that the quantity $\frac{\partial}{\partial u} \frac{d^2 H_u}{dt^2}$ can be expressed as:

$$\frac{\partial}{\partial u} \frac{d^2 H_u}{dt^2}(t) = \frac{(s_{in}^1 - s_1(t))(s_{in}^1 + s_{in}^2 - s_1(t) - s_2(t))}{\det(f(s(t)), g(s(t)))} b(s(t)), \quad t \in [t_1, t_2].$$

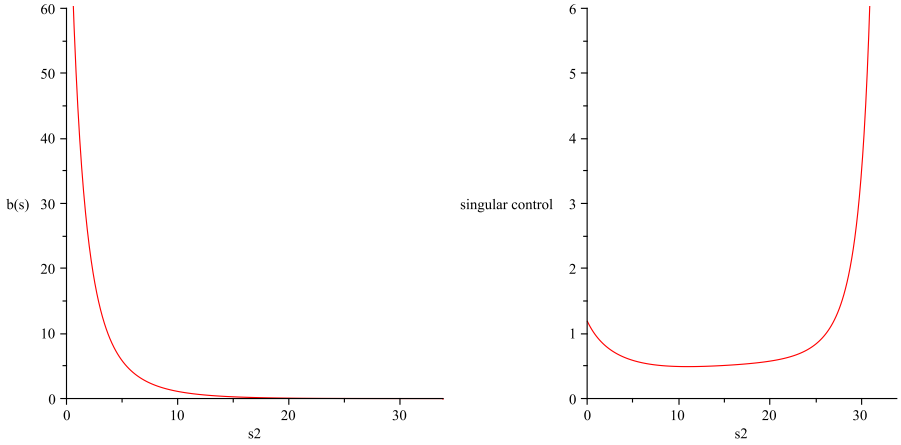

Figure 4: *Picture left* : Plot of the mapping $b(\cdot)$ along the singular locus Δ_{SA} as a function of s_2. *Picture right*: plot of the singular control as a function of s_2.

Hence, this quantity computed on the singular locus is positive in Δ_0^+ and negative in Δ_0^-, which concludes the proof. □

Remark 3.3. *These properties of singular arcs can be also retrieved using the clock form argument. Recall from* [14] *that given two trajectories γ_1 and γ_2, not intersecting Δ_0, and steering a point $z^0 \in \mathcal{D}$ to a point $z^1 \in \mathcal{D}$ in time t_1 and t_2 respectively, one has*

$$t_1 - t_2 = \iint_\Omega \frac{\det(g(s), [f,g](s))}{\det(f(s), g(s))^2}\, \mathrm{d}s,$$

where Ω is the domain enclosed by $\gamma_1 \cup \gamma_2$ oriented counter-clockise (the domain Ω is with a non-empty interior since $\gamma_1 \neq \gamma_2$). Thanks to the expression of $t_1 - t_2$ and to the sign of $\det(g(s), [f,g](s))$ in $\Delta_0^{\pm}$, we retrieve that any singular arc contained in Δ_{SA}^+, resp. in Δ_{SA}^- is a turnpike, resp. an anti-turnpike as in Proposition 3.3.

3.2.3 Extended target set

Since the target point $\bar{s}$ belongs to the curve Δ_0 which contains exactly one steady state singular point, the target $\bar{s}$ can be reached by only two trajectories of (2.7) for the control $u = 0$ or $u = u_{max}$.

It is convenient to introduce an *extended target set* that is constructed from the target point $\bar{s}$ as follows. First, let us define the semi-orbit $\mathcal{C}_0$ by

$$\mathcal{C}_0 := \{s^0(t, \bar{s}) \ ; \ t \in \mathbb{R}_+\},$$

where $s^0(\cdot, \bar{s})$ is the unique solution of (2.7) backward in time with $u = 0$ starting from the target point $\bar{s}$ at time 0. From (2.7), one can show that s^0 satisfies the following property (the proof is postponed into the Appendix in Section 7).

Property 3.3. *The semi-orbit $\mathcal{C}_0$ satisfies*

$$\lim_{t \to +\infty} s^0(t, \bar{s}) = (s_{in}^1, s_{in}^2) \quad \text{and} \quad \lim_{t \to +\infty} \frac{s_{in}^2 - s_2^0(t, \bar{s})}{s_{in}^1 - s_1^0(t, \bar{s})} = +\infty. \tag{3.14}$$

Note that

$$\mathcal{C}_0 \cap (\Delta_0^- \cap \Delta_{SA}^+) = \emptyset, \tag{3.15}$$

since any trajectory starting from Δ_{SA}^+ with $u = 0$ cannot intersect the curve Δ_0 (see also Fig. 3). Similarly, we consider the semi-orbit $\mathcal{C}_1$ (restricted to the set $\mathcal{D}$) defined by:

$$\mathcal{C}_1 := \{s^1(t, \bar{s}) = (s_1^1(t, \bar{s}), s_2^1(t, \bar{s})) \in \mathcal{D} \ ; \ t \in \mathbb{R}_+\}, \tag{3.16}$$

where $s^1(\cdot, \bar{s})$ is the unique solution of (2.7) backward in time with $u = u_{max}$ starting from the target point $\bar{s}$ at time 0.

Definition 3.3. *We call extended target set $\mathcal{T}$ the subset of $\mathcal{D}$ defined by:*

$$\mathcal{T} := \mathcal{C}_0 \cup \mathcal{C}_1. \tag{3.17}$$

Depending on the position of $\bar{s}$ on the curve Δ_0, the curve $\mathcal{C}_1$ can exit the domain $\mathcal{D}$ through the axis $\{s_2 = 0\}$ (see Fig. 7 and 9) or $\{s_1 = 0\}$ (see Fig. 10). Moreover, $\mathcal{T} \cap \Delta_0$ consists of two points $\bar{s}$ and $\bar{s}'$ (see Fig. 7 and 9) except when $\bar{s} = s^\star$ (in the latter, $\mathcal{T} \cap \Delta_0$ consists of only one point, see Fig. 8).

If $\mathcal{C}_1$ exits the domain $\mathcal{D}$ through the axis $\{s_1 = 0\}$, then we set $s_1^e := 0$ and $s_2^e := s_2^1(t_e, \bar{s})$ where t_e is the first exit time of $s_1(\cdot, \bar{s})$ of $\mathcal{D}$. Otherwise let $s_1^e \in (0, s_{in}^1)$ the value of s_1 for the unique intersection point between $\mathcal{C}_1$ and the axis $\{s_2 = 0\}$. The point $(s_1^e, 0)$ corresponds to the exit point of $\mathcal{C}_1$ of the set $\mathcal{D}$, and in this case we set $s_2^e := 0$. Since one has $\dot{s}_1 < 0$ along $\mathcal{C}_0$ and $\dot{s}_1 > 0$ along $\mathcal{C}_1$, the curve $\mathcal{T}$ can be written as the graph of a continuous function

$$s_1 \mapsto s_2 := \xi(s_1), \quad s_1 \in [s_1^e, s_{in}^1]$$

with $\xi(s_1^e) = s_2^e$ and $\xi(s_{in}^1) = s_{in}^2$. It follows that the set $\mathcal{T}$ partitions $\mathcal{D}$ into two connected subsets A and B defined by:

$$A := \{s = (s_1, s_2) \in \mathcal{D} \ ; \ s_2 > \xi(s_1)\} \quad \text{and} \quad B := \{s = (s_1, s_2) \in \mathcal{D} \ ; \ s_2 < \xi(s_1)\}. \tag{3.18}$$

This partition of $\mathcal{D}$ (roughly speaking above and below $\mathcal{T}$) will be useful to state the optimal synthesis in the next section.

3.2.4 Numerical computation of the target point

We conclude this section by a numerical computation of the target point $\bar{s} = (\bar{s}_1, \bar{s}_2)$ maximizing the static biogas production using the numerical values in [5]. Following Proposition 2.1, the target point $(\bar{x}_1, \bar{s}_1, \bar{x}_2, \bar{s}_2)$ that maximizes the quantity $\mu_2(s_2)x_2$ among steady states of (2.1) is such that $\bar{x}_1 > 0$ and $\bar{x}_2 > 0$. Such equilibrium point satisfies

$$\mu_1(\bar{s}_1) = \mu_2(\bar{s}_2) = u \quad \text{and} \quad \bar{x}_2 = s_{in}^1 + s_{in}^2 - \bar{s}_1 - \bar{s}_2.$$

Note that the equation $\mu_2(s_2) = u$ admits at most two solutions and $\bar{s}_2$ denotes the smallest one. As a consequence, the target point is obtained by maximizing the function (with respect to constant values of u)

$$u \mapsto p(u) := u(s_{in}^1 + s_{in}^2 - \mu_1^{-1}(u) - \mu_2^{-1}(u)), \quad u \in [0, \mu_2(s_{max})],$$

where for a given $u \geq 0$, $\mu_2^{-1}(u)$ is the smallest solution of the equation $\mu_2(\bar{s}_2) = u$. The graph of p is depicted on Figure 5 and we find numerically that

$$\bar{s} := (4.59, 6.75). \tag{3.19}$$

Finally, Figure 6 summarizes the main geometrical features of the system (collinearity curve, singular arc, and extended target) in the case where the target point is given by (3.19).

4 Optimal synthesis

In this part, we provide an optimal feedback control for (2.12) in the domain $\mathcal{D}$ by decomposing this set into the three subsets A, B (defined by (3.18)), and $\mathcal{T}$ (defined by (3.17)). Due to the different behavior of singular arcs in the sets Δ_0^- and Δ_0^+ (see Proposition 3.3), the optimal synthesis will be slightly different in both sets A and B. As a byproduct of this study, we will obtain the controllability of the target *i.e.* for any $\bar{s} \in \Delta_0$, we will describe the set of initial conditions $s^0 \in \mathcal{D}$ for which there exists an admissible control steering (2.7) from s^0 to $\bar{s}$.

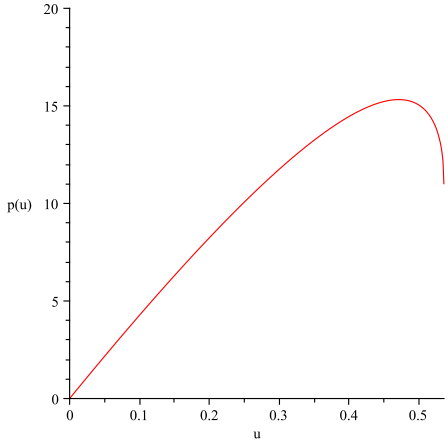

Figure 5: Plot of the function $u \mapsto p(u)$. The maximum is achieved for $u = 0.47$.

4.1 Optimal synthesis on the extended target $\mathcal{T}$

We start by stating the following useful property on the behavior of trajectories of (2.7) with the constant control $u = u_{max}$ (it is in line with Property 3.3).

Property 4.1. *Given $s^0 \in \mathcal{D}$, let $s(\cdot)$ be the unique solution of (2.7) with the control $u = u_{max}$. Then one has*

$$\lim_{t\to+\infty} s(t) = (s^1_{in}, s^2_{in}) \quad \text{and} \quad \lim_{t\to+\infty} \frac{s^2_{in} - s_2(t)}{s^1_{in} - s_1(t)} = -1. \tag{4.1}$$

For brevity, the proof has been postponed into the Appendix. We now prove that for any initial condition belonging to the extended target set $\mathcal{T}$, it is optimal to stay on this set.

Proposition 4.1. *If s^0 is an initial condition in $\mathcal{C}_0$, resp. $\mathcal{C}_1$, then the optimal control is $u = 0$, resp. $u = u_{max}$ until reaching $\bar{s}$.*

Proof. We consider an initial condition $s^0 \neq \bar{s}$ on the curve $\mathcal{C}_0$ and we suppose by contradiction that it has a switching point from $u = 0$ to $u = u_{max}$ at a time t_c before reaching $\{\bar{s}\}$. Note that by construction of the extended target set, then $s(t_c) \notin \Delta_0^- \cap \Delta_{SA}^+$ (recall (3.15)). We now consider the three following cases depending on the location of $s(t_c)$ on the curve $\mathcal{C}_0$.

First case. We assume that $s(t_c) \in \Delta_0^- \cap \Delta_{SA}^-$ or $s(t_c) \in \Delta_0^+ \cap \Delta_{SA}^+$. Then, we have $\dot{\phi}(t_c) \geq 0$ which contradicts that $\dot{\phi}(t_c) = -\theta(s(t_c)) < 0$ (recall Proposition 3.1 (ii)). Hence, this case is not possible.

Second case. Suppose that $s(t_c) \in \Delta_0^+ \cap \Delta_{SA}^-$. Then, the trajectory cannot switch from $u = u_{max}$ to $u = 0$ in $\Delta_0^+ \cap \Delta_{SA}^-$ at some time $t > t_c$ (recall Proposition 3.1 (ii)). Thus, it necessarily exits the set Δ_0^+ entering into $\Delta_0^- \cap \Delta_{SA}^-$ (indeed, trajectories with $u = u_{max}$ cross Δ_0 in Δ_{SA}^- only). The trajectory necessarily has another switching point $t_c' > t_c$ from $u = u_{max}$ to $u = 0$ (otherwise it does not reach the target). We conclude that it would have two switching points in Δ_0^+ and Δ_0^- which contradicts Lemma 3.2. Hence, this case is not possible.

Third case. Finally, we suppose that it has a switching point at a time t_c from $u = 0$ to the singular locus (if this case is possible depending on the position of $\bar{s}$ with respect to $s^\star$). Then, one necessarily has $s(t_c) \in \Delta_0^+ \cap \Delta_{SA}$. Moreover, the corresponding singular trajectory must have a second switching point (otherwise it converges asymptotically to $s^\star$ and it does not reach the target). Hence, the trajectory necessarily switches either to $u = 0$ or to $u = u_{max}$ in the set B. Again from Proposition 3.1 (ii), we deduce that the trajectory necessarily enters into the set Δ_0^- either with $u = 0$ or $u = u_{max}$. In both cases, the trajectory does not reach the target if it does not contain a switching point in Δ_0^-. Hence, we have a contradiction as it would have two switching points in Δ_0^+ and Δ_0^-. Thus, this case is not possible.

To conclude, we have proved that for any initial condition in $\mathcal{C}_0$, an optimal control consists in taking $u = 0$ until reaching $\bar{s}$. Similar arguments show that for any initial condition on the curve $\mathcal{C}_1$, then the optimal control is $u = u_{max}$ until reaching $\bar{s}$. □

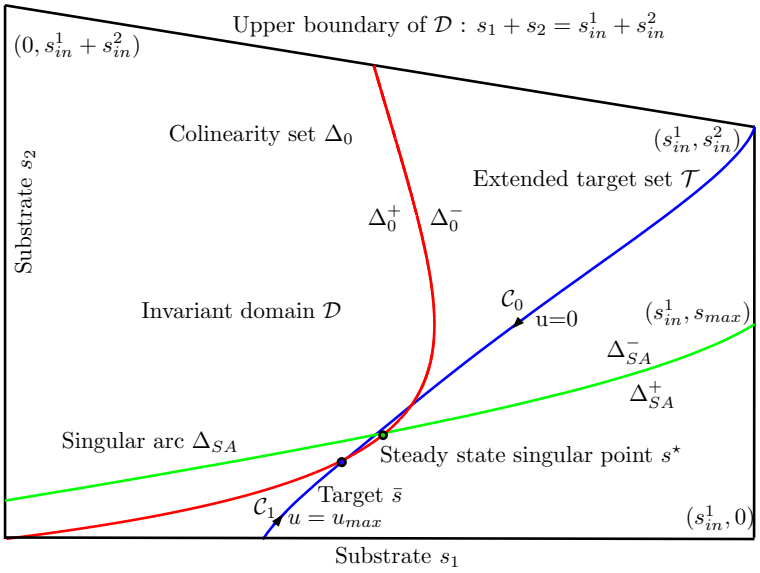

Figure 6: Main characteristics of system (2.7) : Invariant domain $\mathcal{D}$, collinearity set Δ_0 (together with $\Delta_0^{\pm}$), singular locus Δ_{SA} (together with $\Delta_{SA}^{\pm}$), extended target $\mathcal{T} = \mathcal{C}_0 \cup \mathcal{C}_1$.

4.2 Optimal synthesis in the set A

In this section, we introduce a feedback control[5] $u[\cdot,\cdot]$ defined in the set A by:

$$u[s_1, s_2] := \begin{cases} 0 & \text{if} \quad s_1 < \delta_{SA}(s_2), \\ u_s(s_2) & \text{if} \quad s_1 = \delta_{SA}(s_2), \\ 1 & \text{if} \quad s_1 > \delta_{SA}(s_2). \end{cases} \tag{4.2}$$

Hereafter, we shall refer to the singular arc strategy (SAS) for the operation of the feedback control (4.2) on the system (2.7). In the set A, we have the following optimality result (see Figure 7).

Proposition 4.2. *Suppose that* (3.13) *holds true. Then, for any* $\bar{s} \in \Delta_0$ *such that* $\bar{s} \neq s^\star$, *the feedback control* (4.2) *drives optimally any initial condition in* A *to the extended target set* $\mathcal{T}$.

Proof. First, let us recall that the singular locus Δ_{SA} restricted to Δ_0^+ is time minimizing *i.e.* any singular arc contained in this set is locally optimal (see Proposition 3.3). Moreover such arcs are non-saturating from (3.13).

Now, since $\bar{s} \neq s^\star$, we have the following cases:
First case. Consider an initial condition $s^0 \in \Delta_0^+ \cap \Delta_{SA}^-$. Then, if one has $u = u_{max}$, the trajectory must exit the set Δ_0^+ (recall Proposition 3.1 (ii)) and it necessarily enters into the set Δ_0^-. In that case, the trajectory cannot reach the extended target $\mathcal{T}$ with $u = u_{max}$, thus it must have a first switching point to $u = 0$ in Δ_0^-. If the trajectory reaches the target point, it necessarily also has a switching point in the set Δ_0^+ since the target set $\mathcal{T}$ cannot be reached from the set $A \cap \Delta_0^-$. We thus have a contradiction as the trajectory contains switching points both in Δ_0^+ and Δ_0^-. This shows that we must have $u = 0$ until reaching the singular arc.
Second case. Consider an initial condition $s^0 \in \Delta_0^- \cap \Delta_{SA}^-$. If one has $u = u_{max}$ at time $t = 0$, then the trajectory must have a switching point in Δ_0^- (since this trajectory converges to the point (s_{in}^1, s_{in}^2) without intersecting $\mathcal{T}$ in Δ_0^-) and, as it reaches the target, it must also have a switching point in Δ_0^+ (as in the previous case) which contradicts Lemma 3.2. Thus, we necessarily have also $u = 0$ in $\Delta_0^- \cap \Delta_{SA}^-$.

This proves that the optimal control is $u = 0$ in the set $\Delta_{SA}^- \cap A$. Similar arguments show that the optimal control is $u = u_{max}$ in the set $\Delta_{SA}^+ \cap A$. Moreover, singular trajectories are optimal until reaching $\mathcal{T}$, otherwise there would exist a time t where a singular trajectory leaves the singular locus in Δ_0^+ either with $u = 0$ or

[5]The notation $u[s_1, s_2]$ indicates that u is a feedback control that depends on the state variable whereas $u(\cdot) \in \mathcal{U}$ denotes an open loop control.

with $u = u_{max}$. We would obtain a contradiction using the previous analysis. Hence, to remain in the singular locus is optimal until reaching $\mathcal{T}$. □

Remark 4.1. *If $\bar{s} = s^\star$ the target point is not reachable from initial conditions in A. Indeed, we know that $\mathcal{T}$ is tangent to Δ_0 at $s^\star$ (see e.g. [3]). Thus, one has $\mathcal{T} \setminus \{\bar{s}\} \subset \Delta_0^-$ since $\Delta_0 \cap \Delta_{SA}$ is reduced to a singleton and $\lim_{t\to+\infty} s^0(t, \bar{s}) = (s_{in}^1, s_{in}^2)$ (see (3.14)). Note also that singular trajectories reach the point $s^\star$ in infinite horizon, thus any trajectory reaching $\mathcal{T}$ from the set A necessarily reaches $\mathcal{C}_0\backslash\{s^\star\}$ with $u = u_{max}$ or $\mathcal{C}_1\backslash\{s^\star\}$ with $u = 0$. Hence, the trajectory must have a switching point from $u = u_{max}$ to $u = 0$ on $\mathcal{C}_0\backslash\{s^\star\}$ or from $u = 0$ to $u = u_{max}$ on $\mathcal{C}_1\backslash\{s^\star\}$. Moreover, it belongs to the set A in a left neighborhood of such a switching point. This is a contradiction with Proposition 3.1 (ii) as $\mathcal{T}\backslash\{\bar{s}\} \subset \Delta_0^-$. Hence, the target point cannot be reached from A when $\bar{s} = s^\star$.*

Remark 4.2. *Proposition 4.2 shows that optimal trajectories starting from A should reach the singular locus in minimal time and stay on this set until reaching the extended target set $\mathcal{T}$. This optimal strategy in the set A illustrates the turnpike property of the singular locus in Δ_0^+ (see Figure 7) established in Proposition 3.3. As a byproduct, we also obtain that the set $A \cup \mathcal{T}$ is optimally invariant (even though A is non-necessarily invariant by (2.7)).*

4.3 Optimal synthesis in the set B and cut-locus

We first, verify that the target point $\bar{s}$ can be reached by any point in the set B.

Lemma 4.1. *The target set can be reached from any initial condition $s^0 \in B$.*

Proof. Recall from Property 3.3 that $\lim_{t\to+\infty} s^0(t, \bar{s}) = (s_{in}^1, s_{in}^2)$ and $\lim_{t\to+\infty} \frac{s_{in}^2 - s_2^0(t,\bar{s})}{s_{in}^1 - s_1^0(t,\bar{s})} = +\infty$. In view of (4.1), the unique solution of (2.7) with $u = u_{max}$ starting from a given initial condition $s^0 \in B$ necessarily intersects $\mathcal{C}_0$ in finite time which ends the proof (the target $\bar{s}$ can be reached from any point of $\mathcal{C}_0$). □

First, it can be observed that optimal trajectories starting in the set B should necessarily reach the extended target set $\mathcal{T}$ before reaching $\bar{s}$. Hence, the set $B \cup \mathcal{T}$ is also optimally invariant utilizing Proposition 4.1.

Due to the anti-turnpike property of the singular locus in Δ_0^-, the optimal synthesis will be slightly different in the set B : the singular locus in Δ_0^- is time maximizing, therefore optimal trajectories do not take advantage of staying on the singular arc. Instead, they should reach the extended target set in minimal time with an extremal value for the control in such a way to stay far from the singular locus. In the case of a time maximizing singular arc, extremal trajectories can switch alternatively in the sets $\Delta_{SA}^+ \cap \Delta_0^-$ and $\Delta_{SA}^- \cap \Delta_0^-$. Nevertheless, optimal trajectories are the extremal trajectories with the minimum number of switching times. Indeed, for the point to point minimal time control problem, Proposition 27 of [6] (see also [8, 24, 23, 22]) implies that in the case of an elliptic singular arc (*i.e.* time maximizing), then optimal trajectories have at most one switching point before reaching $\{\bar{s}\}$ in a neighborhood of the singular locus. Hence, if we denote by $B_\pm$ a Bang arc with $u = 0$ or $u = u_{max}$, we can expect that optimal trajectories in the set B are of two types: for each initial condition $s^0 \in B$, either the control $u = u_{max}$ until reaching $\mathcal{T}$ is optimal or the control $u = 0$ until reaching $\mathcal{T}$ is optimal. Let us then introduce two functions $s^0 \mapsto v_{10}(s^0)$, $s^0 \mapsto v_{01}(s^0)$ in the set B as follows:

- The time of the strategy B_+B_- from a given initial condition $s^0 \in B$ (*i.e.* $u = u_{max}$ until reaching $\mathcal{C}_0$ and then $u = 0$ until reaching $\bar{s}$) is denoted by $v_{10}(s^0)$.
- The time of the strategy B_-B_+ from a given initial condition $s^0 \in B$ (*i.e.* $u = 0$ until reaching $\mathcal{C}_1$ and then $u = u_{max}$ until reaching $\bar{s}$) is denoted by $v_{01}(s^0)$.

It follows that optimal trajectories may be non unique depending if the mapping $s^0 \mapsto v_{10}(s^0) - v_{01}(s^0)$ vanishes in the set B or not.

Definition 4.1. *A cut-locus $\mathcal{L}$ is defined as the set of points where the optimal feedback is non-unique.*

In our setting, the cut-locus then separates the set B into two subsets where in each subset, the strategy B_+B_- and B_-B_+ are optimal respectively. Moreover, for any initial condition in $\mathcal{L}$, both trajectories B_+B_- and B_-B_+ reach $\bar{s}$ in the same time *i.e.* one has $v_{10}(s^0) = v_{01}(s^0)$. The computation of this locus has been performed using a homotopy method.

Note that when $s_1^e = 0$, then, the strategy B_-B_+ is not admissible (in that case, any solution of (2.7) for the control $u = 0$ starting in B cannot intersect the curve $\mathcal{C}_1$). Hence, $\mathcal{L} = \emptyset$ and only the strategy B_+B_- is optimal until reaching the target point $\bar{s}$, see Figure 10.

4.4 Full synthesis

The following Theorem provides the optimal synthesis for problem (2.12) and summarizes the previous results obtained in the sets A and B.

Theorem 4.1. *Suppose that $\Delta_0 \cap \Delta_{SA}$ is reduced to a singleton $\{s^\star\}$, that Δ_{SA} is simply connected, and let $\bar{s} \in \Delta_0$ be a target point. In addition, suppose that* (2.6), (3.7) *and* (3.13) *hold true. Then, one has the following optimality results.*

(i) If $\bar{s} = s^\star$, then the target set can be reached from initial conditions in the set B only.

(ii) If $\bar{s} \neq s^\star$, then the target set can be reached from any initial conditions in the set $\mathcal{D}$.

(iii) For any $\bar{s} \in \Delta_0$, an optimal feedback control for (2.12) *is given as follows:*

- *For any initial condition on $\mathcal{C}_0$, resp. $\mathcal{C}_1$, an optimal control is $u = 0$, resp. $u = u_{max}$ until reaching $\mathcal{T}$.*
- *In the set A, the optimal strategy is SAS and the feedback control* (4.2) *drives optimally any initial condition $s^0 \in A$ to the set $\mathcal{T}$.*
- *In the set B, from any initial condition, either the strategy $B_- - B_+$ or $B_+ - B_-$ is optimal depending on the initial condition with respect to the cut-locus $\mathcal{L}$ (if it exists).*

Remark 4.3. *It is worth noting that the optimal synthesis will be similar if the target point $\bar{s}$ is not in the collinearity set Δ_0. We do not develop this case because in our problem, the target point is the steady state that maximizes the biogas flow rate at equilibrium and, under our assumptions, this point is in Δ_0.*

5 Conclusion

In this paper, we provided an optimal feedback control of Problem (2.12) that allows to reach in minimal time the target point maximizing the biogas production at steady state. To do so, we defined an extended target set that enabled us to decompose the state space into two subsets A and B and give the optimality results in each subset. It is worth to mention that the structure of the optimal control is different in A and B due to the turnpike and anti-turnpike properties of the singular arc in the two subsets $\Delta_0^{\pm}$.

The optimality results mainly rely on the geometry of the collinearity curve Δ_0 and of the singular locus Δ_{SA}, and more precisely on the fact that $\Delta_0 \cap \Delta_{SA}$ is reduced to a singleton separating Δ_{SA} into a turnpike and an anti-turnpike. If more than two steady state singular points appear, the study of global optimality results would be more intricate and out of the scope of the paper. Let us point out that our methodology allows to treat quite general minimal time control problems having this particular structure (*i.e.* one steady state singular point in the invariant domain together with a turnpike and an anti-turnpike for the singular locus, see *e.g.* [3, 7]).

From a practical point of view, the determination of an autonomous feedback control is useful to drive optimally the control system to the optimal target point at steady state (it is in particular robust to control the system if uncertainties affect the process). Moreover, the knowledge of the different curves Δ_0, Δ_{SA}, and $\mathcal{L}$ may be useful to increase the performance of a fermentor operated by the synthesized feedback control. In particular, depending on the position of the initial condition w.r.t. these curves, one can then choose an adequate control policy driving the system to the target point. It is also worth to mention that this control law can also be used as a sub-optimal strategy (for the time criterion) in the case when initial conditions are no longer on the set $\mathcal{V}$ or when $\alpha \neq 1$. Since uncertainties can affect the process, the target may be not known exactly on the curve Δ_0, nevertheless, our analysis provides an optimal feedback control for any target point on Δ_0.

6 Acknowledgments

The authors are grateful to Jérôme Harmand, Alain Rapaport and Victor Riquelme for helpful discussions on the subject, and to Aurélien Binet for having contributed to the determination of the cut-locus. The first author would like to thank INRA Montpellier and the UMR MISTEA for providing him a half year delegation during the academic year 2017-2018. This research benefited from the support of FONDECYT grant (Chile) N 1160567 and Proyecto Redes 150011 (Chile). The third author was also partially supported by Basal Project CMM Universidad de Chile.

References

[1] T. Bayen and P. Gajardo, *A note on the steady state optimization of the biogas production in a two-stage anaerobic digestion model*, (2017). `https://hal.archives-ouvertes.fr/hal-01586942`.

[2] T. Bayen, J. Harmand, and M. Sebbah, *Time-optimal control of concentration changes in the chemostat with one single species*, Appl. Math. Model., 50 (2017), pp. 257–278.

[3] T. Bayen, A. Rapaport, and M. Sebbah, *Minimal time control of the two tanks gradostat model under a cascade inputs constraint*, SIAM J. Control Optim., 52 (2014), pp. 2568–2594.

[4] B. Benyahia, T. Sari, B. Cherki, and J. Harmand, *Bifurcation and stability analysis of a two step model for monitoring anaerobic digestion processes*, Journal of Process Control, 22 (2012), pp. 1008 – 1019.

[5] O. Bernard, Z. Hadj-Sadok, D. Dochain, A. Genovesi, and J.-P. Steyer, *Dynamical model development and parameter identification for an anaerobic wastewater treatment process*, Biotechnology and bioengineering, 75 (2001), pp. 424–438.

[6] B. Bonnard and M. Chyba, *Singular trajectories and their role in control theory*, vol. 40 of Mathématiques & Applications (Berlin) [Mathematics & Applications], Springer-Verlag, Berlin, 2003.

[7] B. Bonnard, O. Cots, S. J. Glaser, M. Lapert, D. Sugny, and Y. Zhang, *Geometric optimal control of the contrast imaging problem in nuclear magnetic resonance*, IEEE Trans. Automat. Control, 57 (2012), pp. 1957–1969.

[8] B. Bonnard and M. Pelletier, *Time minimal synthesis for planar systems in the neighborhood of a terminal manifold of codimension one*, J. Math. Systems Estim. Control, 5 (1995), p. 22.

[9] U. Boscain and B. Piccoli, *Optimal syntheses for control systems on 2-D manifolds*, vol. 43 of Mathématiques & Applications (Berlin) [Mathematics & Applications], Springer-Verlag, Berlin, 2004.

[10] J.-B. Caillau, O. Cots, and J. Gergaud, *Differential continuation for regular optimal control problems*, Optim. Methods Softw., 27 (2012), pp. 177–196.

[11] L. Cesari, *Optimization—theory and applications*, vol. 17 of Applications of Mathematics (New York), Springer-Verlag, New York, 1983. Problems with ordinary differential equations.

[12] A. Haddon, J. Harmand, H. Ramírez, and A. Rapaport, *Guaranteed value strategy for the optimal control of biogas production in continuous bio-reactors*, in IFAC Word Congress 2017, July 9-14, 2017.

[13] J. Harmand, C. Lobry, A. Rapaport, and T. Sari, *Le chémostat: Théorie mathématique de la culture continue de micro-organismes*, 2017.

[14] H. Hermes and J. P. LaSalle, *Functional analysis and time optimal control*, Academic Press, New York-London, 1969. Mathematics in Science and Engineering, Vol. 56.

[15] A. Kelessidis and A. S. Stasinakis, *Comparative study of the methods used for treatment and final disposal of sewage sludge in european countries*, Waste management, 32 (2012), pp. 1186–1195.

[16] A. Novick and L. Szilard, *Experiments with the chemostat on spontaneous mutations of bacteria*, Proceedings of the National Academy of Sciences, 36 (1950), pp. 708–719.

[17] M. Sbarciog, M. Loccufier, and A. Vande Wouwer, *On the optimization of biogas production in anaerobic digestion systems*, IFAC Proceedings Volumes, 44 (2011), pp. 7150–7155.

[18] M. Sbarciog, M. Loccufier, and A. Vande Wouwer, *An optimizing start-up strategy for a bio-methanator*, Bioprocess and biosystems engineering, 35 (2012), pp. 565–578.

[19] M. Sbarciog, J. A. Moreno, and A. Vande Wouwer, *A biogas-based switching control policy for anaerobic digestion systems1*, IFAC Proceedings Volumes, 45 (2012), pp. 603–608.

[20] H. Schättler and U. Ledzewicz, *Geometric optimal control*, vol. 38 of Interdisciplinary Applied Mathematics, Springer, New York, 2012. Theory, methods and examples.

[21] H. L. Smith and P. Waltman, *The theory of the chemostat*, vol. 13 of Cambridge Studies in Mathematical Biology, Cambridge University Press, Cambridge, 1995. Dynamics of microbial competition.

[22] H. J. Sussmann, *Regular synthesis for time-optimal control of single-input real analytic systems in the plane*, SIAM J. Control Optim., 25 (1987), pp. 1145–1162.

[23] ——, *The structure of time-optimal trajectories for single-input systems in the plane: the C^∞ nonsingular case*, SIAM J. Control Optim., 25 (1987), pp. 433–465.

[24] ——, *The structure of time-optimal trajectories for single-input systems in the plane: the general real analytic case*, SIAM J. Control Optim., 25 (1987), pp. 868–904.

7 Appendix

In this section, we summarize the variable names and the numerical values used in this paper, and we prove Properties 3.3 and 4.1. We also depict the optimal synthesis of the problem.

- Table 1 describes the name of the variables of (1.1).
- Table 2 indicates the changes of variable to transform (1.1) into (2.1).
- Table 3 provides the numerical values for the parameters that were used for simulations (the variables values before the change of variable are taken from [5] and are explained below).

In the original variables (see (1.1)) the kinetics are given by

$$\tilde{\mu}_1(S_1) := \frac{\mu_{1,max} S_1}{S_1 + K_{S_1}} \quad \text{and} \quad \tilde{\mu}_2(S_2) := \frac{\mu_{2,max} S_2}{S_2 + K_{S_2} + \frac{S_2^2}{K_{I_2}}}.$$

with $\mu_{1,max} = 1.2$, $K_{S_1} = 42.14$, $\mu_{2,max} = 0.74$, $K_{S_2} = 9.28$, $K_{I_2} = 256$, $S_{in}^1 = 10$ and $S_{in}^2 = 93.6$ (see [5]). According to the change of variable indicated in Table 2, we find that $\bar{\mu}_1 = \mu_{1,max}$, $k = K_{S_1}$, $\bar{\mu}_2 = \mu_{2,max}$, $k' = \frac{k_1}{k_2} K_{S_2}$, $k'' = \frac{k_1}{k_2} K_{I_2}$. This yields to the numerical values indicated in Table 3. The maximum value for the dilution rate is taken equal to 1 which is in the range of values of [5].

Remark 7.1. *Using the numerical values indicated in Table 3, we can check numerically that the singular arc is always admissible i.e.*

$$|u_s| < 1. \tag{7.1}$$

Indeed, recall that Δ_{SA} is the graph of $s_2 \mapsto \delta_{SA}(s_2)$ for $s_2 \in [\delta_{SA}^{-1}(0), s_{max}]$ (see (3.9)) and that $\delta_{SA}^{-1}(0) \simeq 3.15$ and $s_{max} \simeq 17.33$. Then, $s_2 \mapsto u_s(s_2)$ indeed satisfies (7.1) over $[\delta_{SA}^{-1}(0), s_{max}]$.

Variable name	Signification	unit
X_1	acidogenic bacteria	g/L
S_1	organic substrate	g/L
X_2	methanogenic bacteria	g/L
S_2	Volatile fatty acids	$mmol/L$
k_i, $i = 1, 2, 3$	Yield coefficients	$mmol/g$
S_{in}^1	Input substrate concentration for S_1	g/L
S_{in}^2	Input sustrate concentration for S_2	$mmol/L$
μ_i, $i = 1, 2$	kinetics of the bacteria	d^{-1}
D	Dilution rate	d^{-1}
α	Retention of biomass parameter	

Table 1: Variable names in (1.1)

New variables in system (2.1)	Original variables in system (1.1)
x_1	$k_1 X_1$
s_1	S_1
x_2	$\frac{k_1 k_3}{k_2} X_2$
s_2	$\frac{k_1}{k_2} S_2$
u	αD
s_{in}^1	S_{in}^1
s_{in}^2	$\frac{k_1}{k_2} S_{in}^2$
$\mu_1(s_1)$	$\tilde{\mu}_1(s_1) = \tilde{\mu}_1(S_1)$
$\mu_2(s_2)$	$\tilde{\mu}_2\left(\frac{k_2}{k_1} s_2\right) = \tilde{\mu}_2(S_2)$

Table 2: Change of variables for obtaining (2.1) from (1.1).

Parameter	Value
k_1	42.14
k_2	116.5
k_3	268
$\bar{\mu}_1$	1.2
k	7.1
$\bar{\mu}_2$	0.74
k'	3.36
k''	92.6
s_{in}^1	10
s_{in}^2	33.85
α	1
u_{max}	1

Table 3: Values of the parameters used for simulations after change of variable indicated in Table 2 (see [5]).

Proof of Property 3.3. Let us denote by $(s_1(\cdot), s_2(\cdot))$ the unique solution of (2.7) backward in time with $u = 0$ starting from $\bar{s}$. If we set $y_1 := s_{in}^1 - s_1$ and $y_2 = s_{in}^2 - s_2$, we then find that $(y_1(\cdot), y_2(\cdot))$ satisfy the ordinary differential equation (ODE):

$$\dot{y}_1 = -y_1 \mu_1(s_{in}^1 - y_1) \quad \text{and} \quad \dot{y}_2 = -y_2 \mu_2(s_{in}^2 - y_2) + (\mu_1(s_{in}^1 - y_1) - \mu_2(s_{in}^2 - y_2))y_1.$$

Thus, one obtains that $y_1(t) \to 0$ when $t \to +\infty$. Using that μ_1 and μ_2 are bounded and that $y_1(t)$ goes to zero when $t \to +\infty$, we deduce that $y_2(t) \to 0$ when $t \to +\infty$ (Barbalat's Lemma). Now, a straightforward

computation shows that if $w := \frac{y_2}{y_1}$, one has

$$\begin{aligned}\dot{w} = \frac{\dot{y}_2}{y_1} - \frac{y_2}{y_1}\frac{\dot{y}_1}{y_1} &= -w\mu_2(s_{in}^2 - y_2) + \mu_1(s_{in}^1 - y_1) - \mu_2(s_{in}^2 - y_2) + w\mu_1(s_{in}^1 - y_1),\\ &= [\mu_1(s_{in}^1 - y_1) - \mu_2(s_{in}^2 - y_2)](w+1).\end{aligned}$$

Let us now set $z := w + 1$ and $\eta(t) := \mu_1(s_{in}^1 - y_1(t)) - \mu_2(s_{in}^2 - y_2(t))$ so that z satisfies the ODE

$$\dot{z} = \eta(t)z.$$

By a direct integration, we get $z(t) = z(0)\exp\left(\int_0^t \eta(t)\ \mathrm{d}t\right)$. Note that $\eta(t) \to \mu_1(s_{in}^1) - \mu_2(s_{in}^2)$ when $t \to +\infty$. Moreover, (2.6) implies that $\mu_1(s_{in}^1) > \mu_2(s_{in}^2)$ (note that following [5], one can check that numerical values of the parameters are such that $\mu_1(s_{in}^1) = 0.7$, $\mu_2(s_{in}^2) = 0.51$, and $\mu_1(s_{in}^1) > \mu_2(s_{in}^2)$). Hence, we find that $\eta(t)$ converges to a positive constant $\eta_\infty > 0$ when $t \to +\infty$. Thus, η is not integrable over $[0, +\infty)$ and thus $z(t) \to +\infty$ when $t \to +\infty$. We conclude that $w(t) = \frac{y_2(t)}{y_1(t)} = \frac{s_{in}^2 - s_2(t)}{s_{in}^1 - s_1(t)} \to +\infty$ when t goes to infinity as was to be proved. □

Proof of Property 4.1. Let $(s_1(\cdot), s_2(\cdot))$ be the unique solution of (2.7) with $u = u_{max}$ starting from a given initial condition $s^0 \in B$. If we set $y_1 := s_{in}^1 - s_1$ and $y_2 = s_{in}^2 - s_2$, we then find that $(y_1(\cdot), y_2(\cdot))$ satisfy the ODE

$$\dot{y}_1 = (\mu_1(s_{in}^1 - y_1) - u_{max})y_1 \quad \text{and} \quad \dot{y}_2 = (\mu_2(s_{in}^2 - y_2) - u_{max})y_2 + (\mu_2(s_{in}^1 - y_1) - \mu_1(s_{in}^2 - y_2))y_1.$$

Similarly as in the proof of Property 3.3, we can show that $\lim_{t\to+\infty} s_1(t) = s_{in}^1$ and $\lim_{t\to+\infty} s_2(t) = s_{in}^2$. Let us now set $w := y_2/y_1$. A straightforward computation shows then that one has

$$\dot{w} = [\mu_2(s_{in}^2 - y_2) - \mu_1(s_{in}^1 - y_1)](w+1).$$

Hence, if we define the function z as $z := w+1$, we find that $\dot{z} = \varepsilon(t)z$ where $\varepsilon(t) := \mu_2(s_{in}^2 - y_2(t)) - \mu_1(s_{in}^1 - y_1(t))$. As $\varepsilon(t)$ congerges to a negative value $-\eta_\infty = \mu_2(s_{in}^2) - \mu_1(s_{in}^1) < 0$, we obtain that $z(t)$ goes to zero when $t \to +\infty$. Hence, we get that $w(t) \to -1$ when t goes to infinity as was to be proved.

We finish this appendix with the plot of optimal syntheses, provided in Section 4.4, for different values of the target point $\bar{s}$:

- Fig. 7 depicts the optimal synthesis in the case where the target is the point of Δ_0 maximizing the bio-gas production (see (3.19)).
- Fig. 8 depicts the optimal synthesis in the particular case when $\bar{s} = s^\star \in \Delta_0$ (*i.e.* the target coincides with the steady-state singular point).
- Fig. 9 depicts the optimal synthesis for a target point $\bar{s} \in \Delta_0$ such that $\bar{s}_2 > s_2^\star$ in the case where the extended target $\mathcal{T}$ intersects the axis $s_2 = 0$.
- Fig. 10 depicts the optimal synthesis for a target point $\bar{s} \in \Delta_0$ such that $\bar{s}_2 > s_2^\star$ in the case where $\mathcal{T}$ does not intersect the axis $s_2 = 0$.

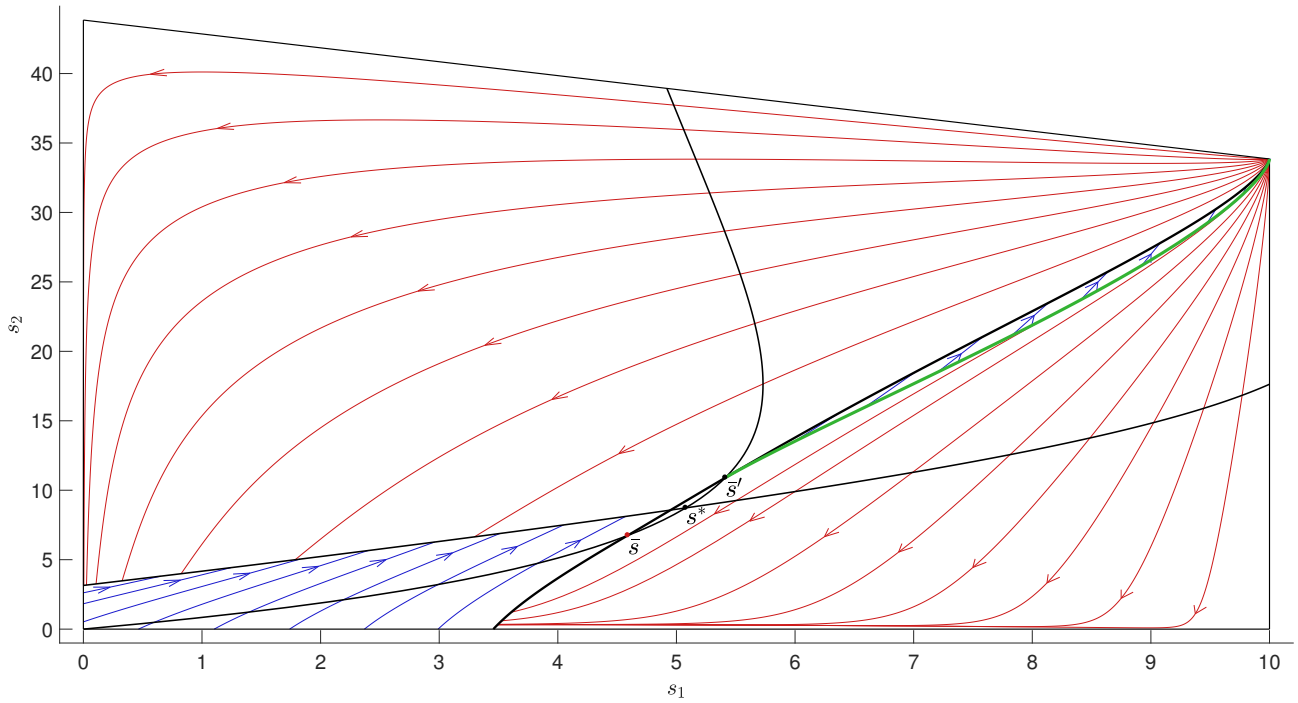

Figure 7: Optimal synthesis for the target point $\bar{s} := (4.59, 6.75)$ maximizing the bio-gas production at steady state. Singular locus, collinearity curve and extended target in black; cut-locus in green. In that case, the cut-locus passes through $\bar{s}'$, the other intersection point between Δ_0 and $\mathcal{T}$.

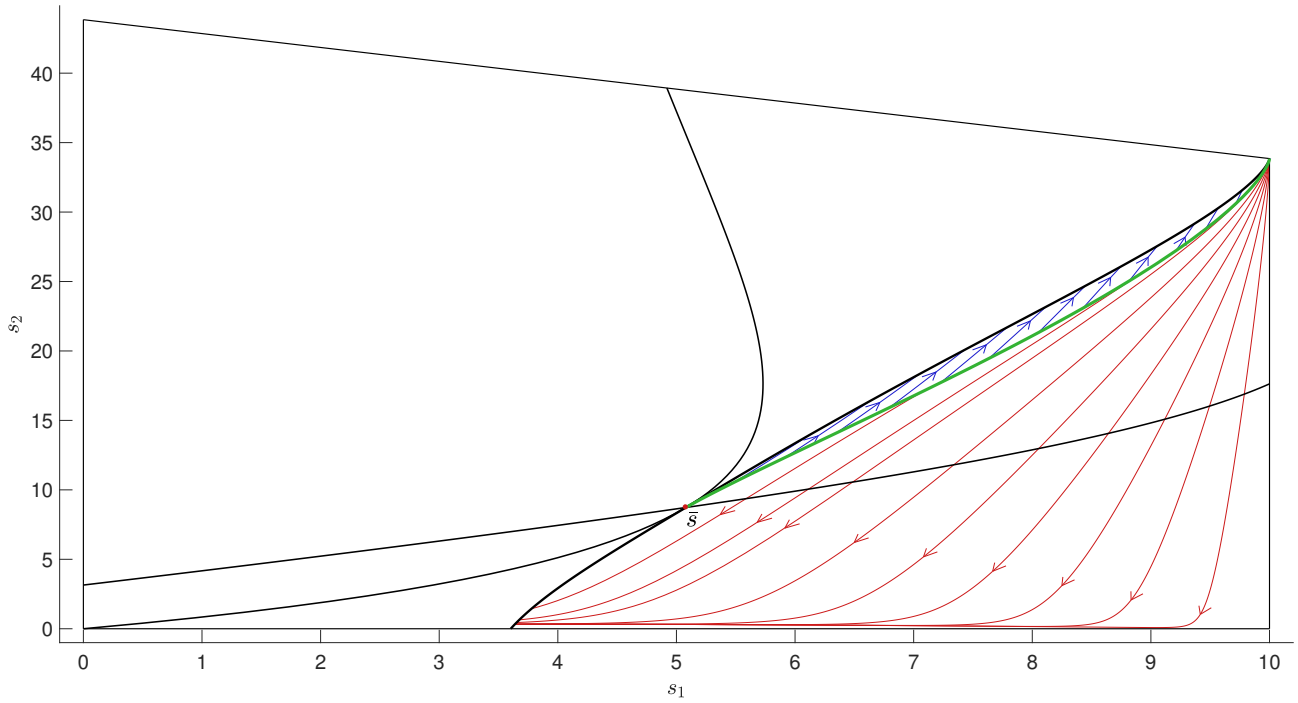

Figure 8: Optimal synthesis when the target point is such that $\bar{s} = s^\star$. Singular locus, collinearity curve and extended target in black; cut-locus in green. In that case, the target set can be reached from the set B only.

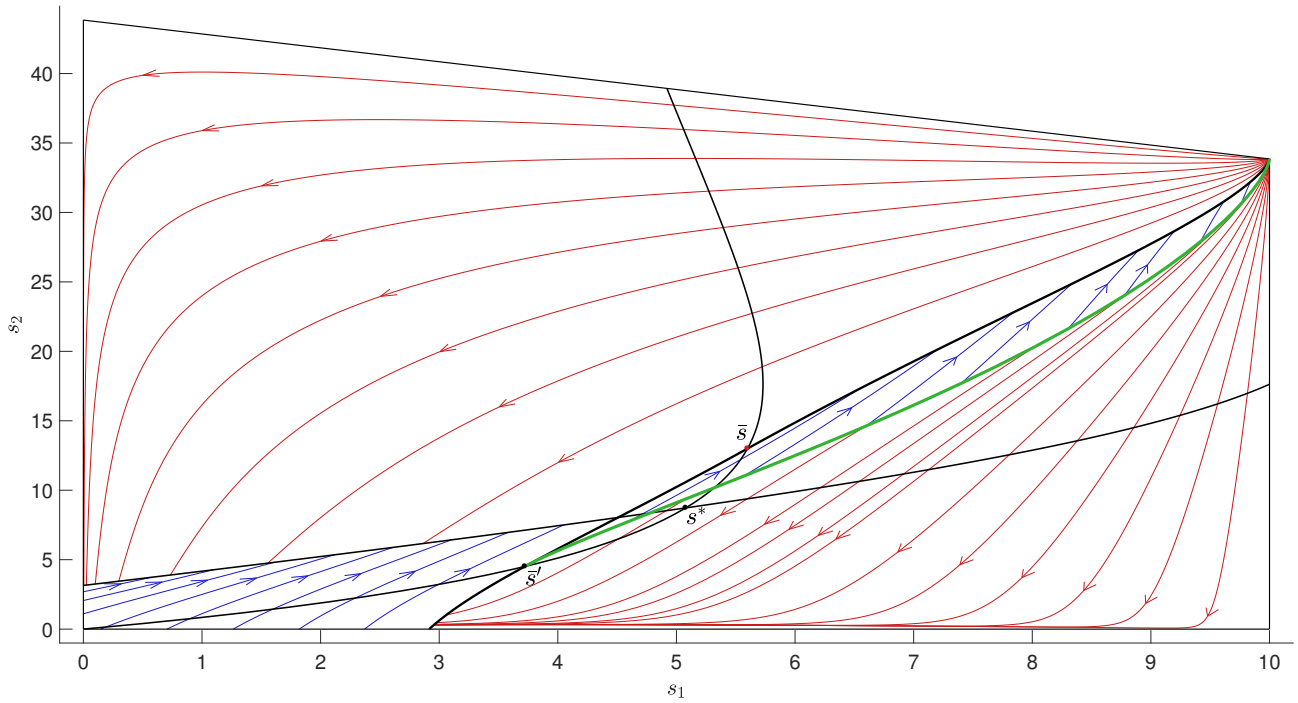

Figure 9: Optimal synthesis for the target point $\bar{s} = (5.52, 12)$. Singular locus, collinearity curve and extended target in black; cut-locus in green. In that case, the cut-locus passes through $\bar{s}'$, the other intersection point between Δ_0 and $\mathcal{T}$.

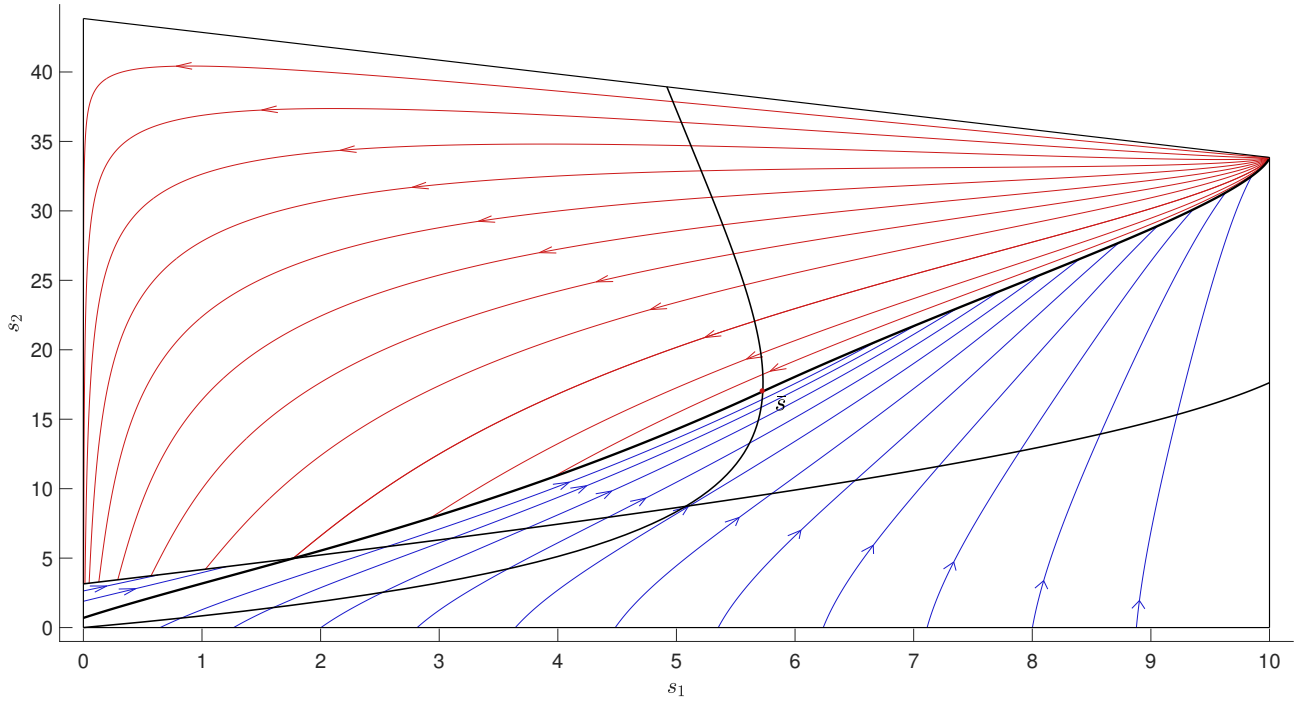

Figure 10: Optimal synthesis for the target point $\bar{s} = (5.72, 17)$. Singular locus, collinearity curve and extended target in black. In that case, the strategy $0-1$ in the set B is not admissible and optimal controls in the set B satisfy $u = 1$.